

Drug target validation of the trypanothione pathway enzymes through metabolic modelling

Viridiana Olin-Sandoval¹, Zabdi González-Chávez¹, Miriam Berzunza-Cruz², Ignacio Martínez³, Ricardo Jasso-Chávez¹, Ingeborg Becker², Bertha Espinoza³, Rafael Moreno-Sánchez¹ and Emma Saavedra¹

¹ Departamento de Bioquímica, Instituto Nacional de Cardiología Ignacio Chávez, México Distrito Federal, Mexico

² Departamento de Medicina Experimental, Facultad de Medicina, Universidad Nacional Autónoma de México, México Distrito Federal, Mexico

³ Departamento de Inmunología, Instituto de Investigaciones Biomédicas, Universidad Nacional Autónoma de México, México Distrito Federal, Mexico

Keywords

control coefficient; drug targeting; kinetic modelling; metabolic control analysis; oxidative stress

Correspondence

E. Saavedra, Departamento de Bioquímica, Instituto Nacional de Cardiología Ignacio Chávez, Juan Badiano No. 1 Col. Sección XVI, Tlalpan, México Distrito Federal 14080, Mexico

Fax: + 5255 55730994

Tel: +5255 5573 2911 ext. 1298

E-mail: emma_saavedra2002@yahoo.com

(Received 12 July 2011, revised 13 February 2012, accepted 1 March 2012)

doi:10.1111/j.1742-4658.2012.08557.x

A kinetic model of trypanothione [T(SH)₂] metabolism in *Trypanosoma cruzi* was constructed based on enzyme kinetic parameters determined under near-physiological conditions (including glutathione synthetase), and the enzyme activities, metabolite concentrations and fluxes determined in the parasite under control and oxidizing conditions. The pathway structure is characterized by a T(SH)₂ synthetic module of low flux and low catalytic capacity, and another more catalytically efficient T(SH)₂-dependent antioxidant/regenerating module. The model allowed quantification of the contribution of each enzyme to the control of T(SH)₂ synthesis and concentration (flux control and concentration control coefficients, respectively). The main control of flux was exerted by γ -glutamylcysteine synthetase (γ ECS) and trypanothione synthetase (TryS) (control coefficients of 0.58–0.7 and 0.49–0.58, respectively), followed by spermidine transport (0.24); negligible flux controls by trypanothione reductase (TryR) and the T(SH)₂-dependent antioxidant machinery were determined. The concentration of reduced T(SH)₂ was controlled by TryR (0.98) and oxidative stress (–0.99); however, γ ECS and TryS also exerted control on the cellular level of T(SH)₂ when they were inhibited by more than 70%. The model predicted that in order to diminish the T(SH)₂ synthesis flux by 50%, it is necessary to inhibit γ ECS or TryS by 58 or 63%, respectively, or both by 50%, whereas more than 98% inhibition was required for TryR. Hence, simultaneous and moderate inhibition of γ ECS and TryS appears to be a promising multi-target therapeutic strategy. In contrast, use of highly potent and specific inhibitors for TryR and the antioxidant machinery is necessary to affect the antioxidant capabilities of the parasites.

Database

The glutathione synthetase gene sequences from the Ninoa and Queretaro strains have been submitted to the GenBank database under accession numbers [HQ398240](#) and [HQ398239](#), respectively

Abbreviations

CumOOH, cumene hydroperoxide; γ EC, γ -glutamylcysteine; γ ECS, γ -glutamylcysteine synthetase; nsGPxA, non-selenium glutathione peroxidase A; GSH, glutathione; GSSG, glutathione disulfide; GS, glutathione synthetase; MCA, metabolic control analysis; Put, putrescine; Spd, spermidine; SpdT, spermidine transport; t-butOOH, *tert*-butylhydroperoxide; TryR, trypanothione reductase; TryS, trypanothione synthetase; T(SH)₂, trypanothione; TS₂, trypanothione disulfide; TXN, tryparedoxin; TXNPx, tryparedoxin peroxidase.

Introduction

The trypanosomatid parasite *Trypanosoma cruzi* is the causal agent of American trypanosomiasis (Chagas disease), which affects 15 million people in Latin America; 28 million people in the endemic countries are at risk of being infected by the parasite [1]. In recent years, Chagas disease has become a worldwide health problem as a result of globalization, with > 300 000 infected people in the USA and > 80 000 in Europe [2]. The current drugs used for treatment of this disease are nifurtimox and benznidazole [3]. However, these compounds are highly toxic to the patient and are effective in the acute phase but not for long-term infections; the emergence of drug-resistant parasite strains is also a problem [4,5]. Thus, there is an urgent need for development of new drugs, and the search and validation of drug targets continue.

In the trypanosomatid human parasites *T. cruzi*, *Trypanosoma brucei* (which causes African trypanosomiasis) and different species of *Leishmania* (which causes several forms of leishmaniasis), the thiol peptide trypanothione (T(SH)₂: N¹,N⁸-bis-glutathionylspermidine), together with the T(SH)₂-dependent antioxidant machinery (tryparedoxin, TXN; TXN-dependent peroxidoredoxin, TXNPx; non-selenium glutathione peroxidase A, nsGPxA) and trypanothione reductase (TryR) replace the antioxidant functions performed by glutathione (GSH), GSH-dependent antioxidant enzymes and glutathione reductase in most cells. T(SH)₂ metabolism in *T. cruzi* is outlined in Fig. 1, and has been extensively reviewed elsewhere [6–9]. Because of the remarkable differences in the antioxidant physiology of these parasites, genetic strategies such as generation of conditional knockouts, gene replacement or RNA interference have been used in *T. brucei* and *Leishmania* to validate the suitability of T(SH)₂ pathway enzymes as drug targets (the evaluated enzymes are indicated in Fig. 1). At 80–100% down-regulation, most of the targeted enzymes were found to be essential for parasite survival, infectivity or oxidative stress management [7–9]. Similar analyses have not been reported for *T. cruzi* because genetic methodologies are under development for this parasite [10].

A drawback in the use of genetic approaches to validate drug targets in metabolic pathways is that, in general, strong down-regulation of individual enzymes in any metabolic pathway in the cell results in complete arrest of the pathway flux or cellular function. Therefore, similar phenotypic and metabolic results are expected when almost any component of trypanosomatid T(SH)₂ metabolism is manipulated [9]. In order to achieve similar levels of enzyme inhibition to those

attained by genetic methods in parasites by pharmacological methods, high doses of specific and potent inhibitors are required, with a concomitant increase in toxic side-effects. Accordingly, genetic strategies are very useful in order to discriminate between essential/non-essential genes, but this is not the only property that determines the suitability of an enzyme as a drug target [11]. Suitable drug targets should be enzymes for which low pharmacological inhibition have a high impact on pathway function. From a metabolic regulation perspective, drug targets should be sought among those enzymes that mainly control the pathway flux and/or the concentration of a particular metabolite.

In recent years, analysis of cellular networks has been used for drug target identification instead of focusing on single enzymes/proteins [12–15]. Metabolic control analysis (MCA) is a quantitative approach in systems biology [16] that has demonstrated that control of a metabolic pathway is distributed to various degrees among all the pathway components, making it possible to establish hierarchies within the pathway components: ‘leaders’ are those enzymes that mainly control the pathway, whereas ‘follower’ enzymes are those that have over-capacity for the pathway flux. Common properties of the former are that they are not abundant in cells, are not catalytically efficient, and/or are highly regulated (allosteric enzymes), whereas the latter are generally non-allosteric, very efficient, and highly abundant in cells [12,13,17,18].

MCA quantifies the degree of control that each enzyme has over the pathway flux (flux control coefficient, C_{ai}^J) and over the pathway intermediary concentrations (concentration control coefficient, C_{ai}^X), where J is the pathway flux, X is an intermediary concentration, and a is the activity of pathway enzyme i in the cell [17,18]. The control coefficients are systemic properties, i.e. they cannot be deduced by analysing the kinetic properties of the single enzymes in isolation. Several experimental strategies have therefore been developed to determine the control coefficients of the individual pathway components in order to determine the control structure of a metabolic pathway [18]. One approach is kinetic modelling, which integrates the kinetic properties of the pathway enzymes determined *in vitro* under near-physiological conditions and the concentrations of pathway precursors and enzyme activities determined in cells into an interactive network that reproduces the pathway behaviour under specific cellular metabolic steady states [19,20]. It is worth emphasizing that the purpose of kinetic modelling is not just to replicate pathway behaviour, but to

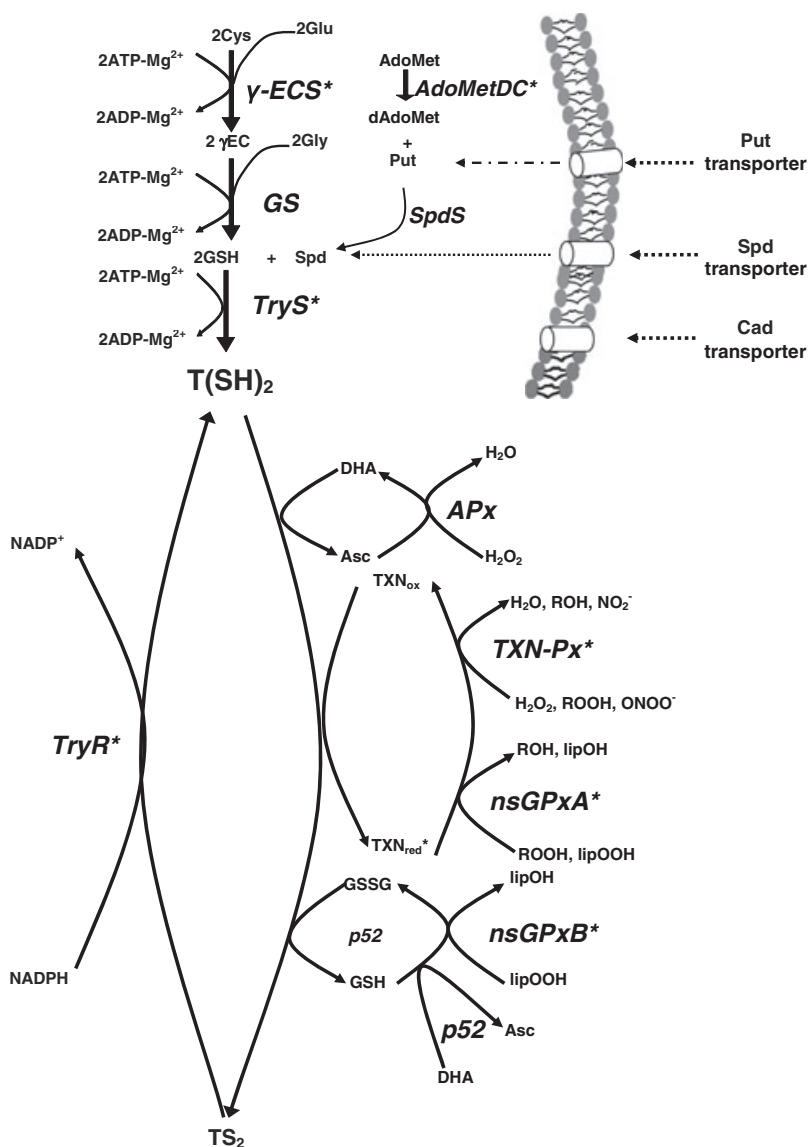


Fig. 1. T(SH)₂ metabolism in *T. cruzi*. T(SH)₂ is synthesized by trypanothione synthetase (TryS, [EC 6.3.1.9](#)) from two GSH molecules and one spermidine (Spd) molecule. In turn, GSH is synthesized by the sequential action of γ -glutamylcysteine synthetase (γ ECS, [EC 6.3.2.2](#)), which binds glutamate (Glu) and cysteine (Cys) to produce γ -glutamylcysteine (γ EC), and glutathione synthetase (GS, [EC 6.3.2.3](#)), which binds γ EC and glycine (Gly) to produce GSH. Six ATP molecules are consumed per mole of T(SH)₂ synthesized. Spd can be *de novo* synthesized by spermidine synthase (SpdS, [EC 2.5.1.16](#)) from putrescine (Put) and decarboxylated-S-adenosyl methionine (dAdoMet); SpdS has only been kinetically characterized in *T. brucei* [83], although the corresponding gene is found in the *T. cruzi* genome. dAdoMet is synthesized from S-adenosylmethionine (AdoMet) by S-adenosylmethionine decarboxylase (AdoMetDC, [EC 4.1.1.50](#)), an enzyme that has been characterized in the three trypanosomatid species (*T. cruzi*, *T. brucei* and *Leishmania*) [70]. In *T. brucei* and *Leishmania*, Put can be *de novo* synthesized by ornithine decarboxylase (ODC, [EC 4.1.1.17](#)) [70]; *Leishmania* can also take up Put from the medium using diamine transporters [84]. *T. cruzi* lacks ODC activity, and therefore relies on transport of Put and Spd from the extracellular environment by high affinity and catalytically efficient diamine/polyamine transporters [65–68]. For the antioxidant system, T(SH)₂ serves as the main electron donor for reduction of oxidized metabolites (dehydroascorbate, DHA; oxidized glutathione, GSSG) and small dithiol proteins (glutaredoxins and trypanredoxin, TXN), which transfer electrons to a variety of antioxidant enzymes such as ascorbate peroxidase (Apx, [EC 1.11.1.11](#)), 2-Cys peroxyredoxins (TXNPx, [EC 1.11.1.15](#)), non-selenium glutathione peroxidase-like enzymes (nsGPxA and nsGPxB, [EC 1.11.1.9](#)) and trypanothione-glutathione thiol transferase (p52). Oxidized trypanothione (TS₂) is regenerated by trypanothione reductase (TryR, [EC 1.8.1.12](#)), consuming NADPH. For reviews, see [6–9]. Asterisks indicate enzymes that were genetically manipulated in *T. brucei* and *Leishmania*.

identify and understand the underlying mechanisms that determine why one enzyme or transporter exerts significant or negligible pathway control [12,13,18–20].

A validated kinetic model of a metabolic pathway may help in the search for suitable drug targets by identifying the steps that exert the greatest control; it can also provide a platform to perform *in silico* experimentation to provide answers to biological questions. Using the kinetic model to assess the impact on fluxes and/or metabolite concentrations of gradual inhibition of each individual pathway component (or simultaneous inhibition of several enzymes in various combinations) allows identification of the step(s) whose inhibition has the greatest negative effect on T(SH)₂ pathway function. Hence, network analysis facilitates prioritization among genetically validated essential enzymes. Moreover, kinetic modelling can also be a valuable tool for drug target validation for parasites for which genetic strategies are limited, such as *T. cruzi*.

Here, we describe construction of the first kinetic model of the T(SH)₂ metabolism in trypanosomatid parasites using *T. cruzi* as a biological model. The kinetic model allowed identification of the enzymes and transporters that exert the greatest control on T(SH)₂ synthesis and concentration and allowed for elucidation of their underlying controlling mechanisms. Moreover, it provided quantitative predictions regarding the degrees of inhibition required for each pathway enzyme to affect antioxidant defence in the parasite.

Results

Due to the significant amount of detailed experimental data required to build kinetic models, only a few have been described, mostly for glycolysis in several organisms (<http://www.biochem.sun.ac.za>; [19]). Although T(SH)₂ metabolism has been thoroughly studied in several laboratories worldwide, the reported data are not uniform: they have been generated using different parasite species and strains, and under diverse experimental conditions. Therefore, to build the kinetic model of T(SH)₂ metabolism in *T. cruzi*, we obtained the majority of the experimental data under near-physiological conditions in the same strain and stage of this parasite species, and under defined metabolic steady states.

***In vitro* kinetic characterization of the recombinant pathway enzymes under near-physiological experimental conditions**

The genes encoding γ -glutamylcysteine synthetase (γ ECS), trypanothione synthetase (TryS), TryR, TXN,

nsGPxA and tryparedoxin peroxidase (TXNPx) of *T. cruzi* Ninoa strain (MHOM/MX/1994/Ninoa) [21] were cloned, and the proteins were over-expressed in *Escherichia coli* and purified to a high degree (approximately 98%) (Fig. S1). The γ ECS and TryS recombinant enzymes were highly unstable under various storage conditions, but the presence of high concentrations of trehalose improved their stabilities, with 50% of the activity lost within 20 days (data not shown).

The intracellular pH of the infective trypomastigote and epimastigote stages have been determined (7.35 and 7.2, respectively [22,23]), and the optimum culture temperatures are 37 and 26 °C, respectively. Therefore, the kinetic parameters of the recombinant enzymes were all determined at pH 7.4 and 37 °C since these conditions more closely resemble the mammalian infective stage.

As previously described, γ ECS, TryS and TryR displayed hyperbolic kinetics for their respective substrates (data not shown), and the kinetic parameter values (Table 1) were within the range reported for several trypanosomatid parasites and other cell types. The latter were mostly determined at 25–37 °C and under optimal pH (7.5–8) (see Table S1 for data comparisons).

Glutathione synthetase (GS) has not been characterized in any trypanosomatid species. Therefore, GS genes were cloned from the *T. cruzi* Ninoa and Querétaro strains (GenBank accessions [HQ398240](#) and [HQ398239](#), respectively), and no differences were found at the level of the amino acid translated sequences. The GS gene was over-expressed in *E. coli*, and the protein purified and kinetically characterized. To improve its poor stability, the enzyme was also stored in trehalose. The enzyme was a dimer (data not shown) that displayed hyperbolic kinetics with its three substrates (Fig. 2). The *TcGS* V_{\max} and K_m values (Table 1) were similar to those reported for GS from *Arabidopsis thaliana* and *Plasmodium falciparum* (Table S1). The enzyme was inhibited by GSH, non-competitively against Gly and ATP and uncompetitively against γ -glutamylcysteine (γ EC) (Fig. 3); however, the three high K_i values (11–14 mM) (Table 1) may not have physiological significance as the GSH concentration in these parasites is one order of magnitude lower (Table 2).

Although the V_{\max} and affinity constants for substrates of *TcTryS* in the Ninoa strain were essentially the same as those of its homologue in the *T. cruzi* Silvio strain (Table S1) [24], the enzyme did not show substrate inhibition by GSH (Fig. S2), as previously reported for the *T. cruzi* Silvio strain recombinant enzyme [24], *T. brucei* [25] and *Leishmania* [26], in

Table 1. Kinetic parameters of recombinant and in the parasite trypanothione pathway enzymes. V_{max} values are units:mg protein⁻¹; K_m , K_m^{app} , K_i and concentrations are mM; k_{cat} , k_{cat}/K_m , V_{max}/K_m values are M⁻¹s⁻¹; V_{max}/K_m^{app} values are mL⁻¹min⁻¹mg protein⁻¹. All values were determined at pH 7.4 at 37 °C in the same buffer (see Experimental procedures). *Values are means ± SD; ** k_{cat} value in s⁻¹ (0.5 for γ ECS, 4.25 for GS, 1.24 for TryS, 983 for TryR, 26 for TXN and 5–10 for TXNPx and nsGPXA); ***values are means ± SEM. Figures in parentheses indicate the number of independent purified protein batches assayed or the number of cytosolic extracts from parasites incubated for 10 min in NaCl/P_i + 20 mM glucose.

Enzyme	Thiol substrate			Co-substrate			Co-substrate/coenzyme			
	V_{max}^* for purified proteins	K_m^{app} *	K_{cat}^{**}/K_m^{app}	K_m^{app} *	K_{cat}^{**}	K_m^{app} *	K_m^{app} *	Inhibitors	V_{max} in parasites***	V_{max}/K_m^{app}
γ ECS	0.37 ± 0.1 (3)	Cys 0.21 ± 0.1 (3)	2.4×10^3	Glu 0.13 ± 0.04 (3)	2.4×10^3	ATP 0.04 ± 0.012 (3)	ATP 0.04 ± 0.012 (3)	$K_{i,GSH}$ 1.6 (2) $K_{i,\gamma EC}$ 0.43 (2) GSSG > 0.003	< 0.002 ^e	< 0.0095
GS	2.04 ± 0.7 (3)	γ EC 0.04 ± 0.01 (3)	1.1×10^5	Gly 1.2 ± 0.3 (3)	1.1×10^5	ATP 0.03 ± 0.01 (3)	ATP 0.03 ± 0.01 (3)	$K_{i,GSH}$ versus Gly 12 ± 0.6 $K_{i,GSH}$ versus ATP 11 ± 1 $K_{i,GSH}$ versus γ EC 14.6 ± 5.6 TS ₂ > 0.005 GSSG > 0.003	0.0086 ± 0.0023 (3)	0.22
TryS ^a	1.04 ± 0.5 (3)	GSH 0.76 ± 0.21 (3)	1.6×10^3	Spd 0.86 ± 0.095 (3)	1.6×10^3	ATP 0.07 ± 0.04 (3)	ATP 0.07 ± 0.04 (3)	Spd, Spm > 2 GSSG > 0.003 T(SH) ₂ > 1 TS ₂ > 0.005	0.0043 ± 0.0016 ^a (3)	0.006
TryR	531 ± 137 (3)	TS ₂ 0.023 ± 0.006 (3)	4.3×10^7	NADPH 0.009 ± 0.005 (3)	4.3×10^7			T(SH) ₂ > 1	0.264 ± 0.087 (3)	11.5
TXN	97 ± 20	T(SH) ₂ 0.092 ± 0.02 (4)	2.8×10^5		2.8×10^5				0.688 (2)	7.5
TXNPx, nsGPXA	1.7–31 ^b	TXN ^b 0.0006–0.0023	$0.14\text{--}6 \times 10^{5c}$	CumOOH ^b 0.011–0.107					0.177 ± 0.0085 ^d (4)	6–16 ^c

^a Activity in μ mol T(SH)₂ synthesized·min⁻¹·mg protein⁻¹. ^b V_{max} and K_m interval of recombinant *T. cruzi* TXNPx and nsGPXA. ^c Calculated using the K_m for CumOOH. ^d Total TXN-dependent peroxidase activity measured using CumOOH. ^e Below the limit of detection of the enzymatic assay. GSSG, oxidized GSH; Spm, spermine.

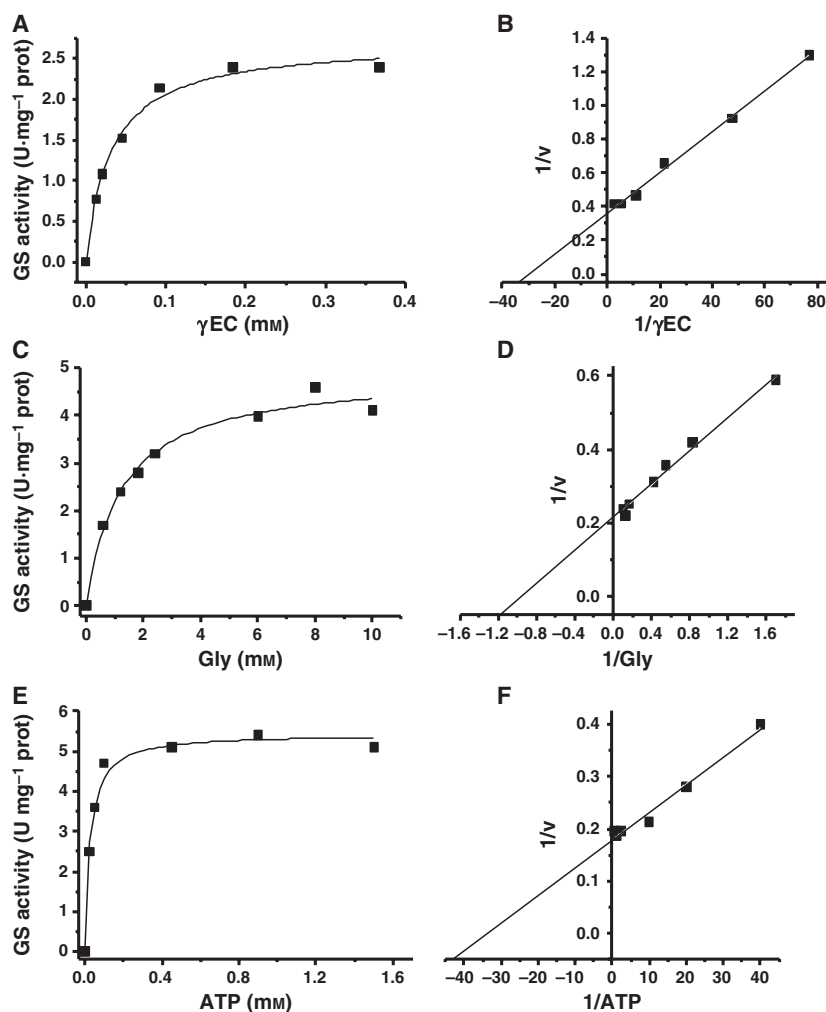


Fig. 2. Kinetic characterization of recombinant *TcGS*. (A,C,E) Titration curves for the three substrates. The fitting of experimental points to the Michaelis–Menten equation was performed using ORIGIN-MICROCAL version 5.0 software (OriginLab; Northampton, MA, USA). The enzyme exhibits hyperbolic kinetics with the three substrates, as shown by the double reciprocal plots (B,D,F).

which inhibition at concentrations of 0.036–1.2 mM was found (Table S1). To evaluate whether the lack of GSH inhibition was an artifact of our recombinant enzyme, TryS activity was determined in parasite cytosol-enriched fractions, i.e. using the native enzyme. Activity was only detected when 6–8 mM GSH was used (10 times the K_m value) (data not shown), suggesting that this high GSH concentration is not inhibitory for *TcTryS* from the Ninoa strain. Furthermore, as a control for our reaction assay, recombinant, His-tagged *Crithidia fasciculata* TryS was partially inhibited at 1 mM GSH. The reason for the lack of *TcTryS* Ninoa inhibition by GSH remains to be elucidated.

The affinity constants of TXN for T(SH)₂, and those of nsGPxA and TXNPx for TXN and cumene peroxide, were determined in a reconstituted system with TryR under the same conditions of pH and temperature used above; the kinetic parameters are shown in Table 1.

The purified enzymes with the lowest catalytic potential ($k_{cat}/K_{m,app}$) regarding the thiol substrate were γECS and TryS; in contrast, efficiencies two to four orders of magnitude higher were obtained for GS, TryR, TXN, nsGPxA and TXNPx (Table 1), indicating that, under *in vitro* saturating concentrations of the thiol substrates, the first two enzymes were less catalytically efficient.

The effect of the products of the enzymatic reactions and some intermediate metabolites of trypanothione metabolism (not usually tested when working with purified enzymes) were evaluated for all the enzymes at concentrations close to those found in these parasites to determine possible regulatory mechanisms when working in the entire pathway (Table 1). γECS was competitively inhibited by GSH and non-competitively by γEC against Glu (Table 1 and Fig. S3). Trypanothione disulfide (TS₂) or T(SH)₂ (0.005 and 1 mM, respectively), glutathione disulfide (GSSG) (0.003 mM), spermidine (Spd) and spermine (2 mM) did not show

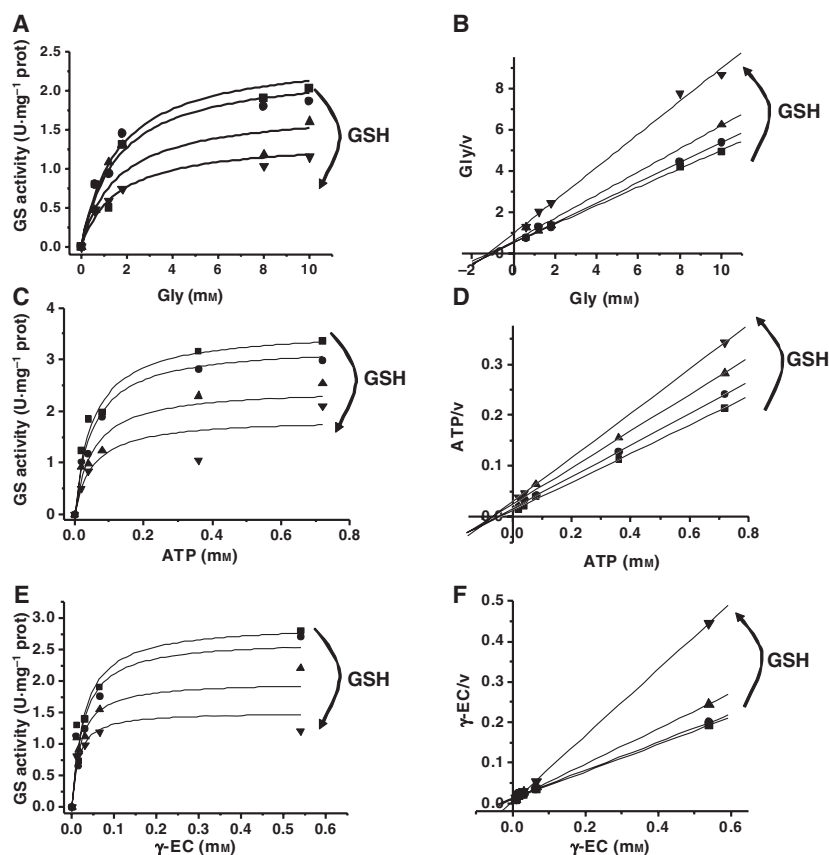


Fig. 3. *TcGS* inhibition by GSH. (A,C) Non-linear curve fitting to the equation for simple non-competitive inhibition $v = (V_{\max}/(1 + I/K_i) * S) / (K_s + S)$. (E) Non-linear curve fitting to the equation for simple uncompetitive inhibition $v = (V_{\max}/(1 + I/K_i) * S) / (K_s/(1 + I/K_i) + S)$ using ORIGINPRO 7.5 software (OriginLab, Northampton, MA, USA). (B,D,F) Hanes' plots corresponding to (A), (C) and (E), respectively. The inhibitor concentration varied from 0 to 10 mM GSH.

Table 2. Metabolomics of the T(SH)₂ pathway in parasites and metabolite concentrations predicted by trypanothione pathway modelling. Simulation of the model setting ¹2.5, ²5 and ³20 μM H₂O₂. *The millimolar concentration was determined on the basis that 10⁸ *T. cruzi* epimastigotes correspond to 3 μL [77]. Values are means ± SD. **Metabolites fixed in the model at the mean value of columns 2, 4 and 6. ***Fluxes (*J*) are in nmol min⁻¹ mg cell protein⁻¹. NI, not included in the model. GSH_{tot} indicates the concentration of reduced *plus* oxidized glutathione.

Incubation (min)	Basal (<i>t</i> = 0)		Control (<i>t</i> = 10)		Stress (<i>t</i> = 10 + stress) (50 μM H ₂ O ₂)	
	<i>In vivo</i>	Model [†]	<i>In vivo</i>	Model [‡]	<i>In vivo</i>	Model [§]
Metabolite (mM)*						
Glu	8.3 ± 1.3 (3)	**	9 ± 1 (3)	**	7.7 ± 1 (3)	**
Gly	13 ± 1.6 (3)	**	9 ± 1.7 (3)	**	12 ± 4 (3)	**
Cys	0.3 ± 0.14 (3)	**	0.4 ± 0.1 ^d (3)	**	0.3 ± 0.07 ^{d,e} (3)	**
γEC	0.15 ± 0.09 (3)	0.067	0.13 ± 0.08 (3)	0.082	0.1 ± 0.04 (3)	0.09
GSH _{tot}	0.8 ± 0.26 (4)	0.68	0.77 ± 0.3 (3)	0.92	0.4 ± 0.05 ^{d,e} (3)	0.5
T(SH) ₂	3.8 ± 1.6 (4)	6.7	5.9 ± 2.5 (4)	7.1	4.2 ± 1.8 ^d (4)	1.7
TS ₂	0.5 ± 0.24 (3)	0.58	0.4 ± 0.22 (3)	0.47	0.6 ± 0.12 (4)	0.34
NADP ⁺	0.039 ± 0.02 (3)	0.026	0.026 ± 0.012 ^f (3)	0.026	0.012 ± 0.004 ^{g,h} (3)	0.025
NADPH	0.12 ^a	0.08	0.084 ^a	0.084	0.04 ^a	0.085
Spd _{int}	1.2 ± 0.06 (3)	0.8	0.2 ± 0.08 ^c (3)	0.33	0.2 ± 0.13 ^c (3)	0.35
Spd _{ext}	0.0011 ^b	**	0.0011 ^b	**	0.0011 ^b	**
ATP	4 ± 0.6 (3)	NI	4.6 ± 0.9 (3)	NI	3.4 ± 1.1 (3)	NI
<i>J</i> _{TrYS} ***		0.88	1 (2)	0.7	1.9 (2)	0.5
<i>J</i> _{TrYR/T(SH)2demand}		252		248		246

^a Recalculated using a NADP/NADPH ratio equal to 0.31 as reported for *T. cruzi* epimastigotes of CL Brener strain [76]. ^b Reported in [82]. Student's *t* tests: ^c *P* < 0.01 versus *t* = 0; ^d *P* < 0.05 versus *t* = 0; ^e *P* < 0.05 versus *t* = 10; ^f *P* < 0.5 versus *t* = 0; ^g *P* < 0.2 versus *t* = 0; ^h *P* < 0.2 versus *t* = 10.

an effect on any of the tested enzymes. No other modulator has been reported to affect any of the T(SH)₂ metabolism enzymes at physiological concentrations. The only allosteric regulatory mechanism that appears to operate in the pathway is that of feedback competitive inhibition by GSH on γ ECS.

Enzyme activities, metabolite concentrations, and fluxes of T(SH)₂ metabolism in parasites

In vivo pathway parameters were determined in *T. cruzi* epimastigotes (insect stage) due to the experimental requirement for large amounts of biological material for reliable determination of enzyme activity or metabolite concentration. This prevented us from performing the analysis in the *T. cruzi* human stages trypomastigotes and amastigotes, for which infection of human cultured cells and further parasite purification are necessary, steps that lead to extremely low parasite yields.

The enzyme activities, metabolite concentrations and fluxes parameters described below were determined under three conditions: in non-incubated parasites (basal $t = 0$), and in parasites incubated for 10 min in NaCl/P_i supplemented with 20 mM glucose in the absence (control $t = 10$) or presence of 50 μ M H₂O₂ ($t = 10+$ stress). At longer incubation times or higher peroxide concentrations (up to 100 μ M), the thiol contents were abruptly depleted, preventing use of such conditions for *in vivo* steady-state experiments.

No simultaneous determination of T(SH)₂ pathway enzyme activities in parasites has been reported, and the V_{\max} values within the cells (i.e. the content of biologically active enzyme) are the most critical kinetic parameters for building kinetic models, because the affinity parameters (K_m , K_A and K_i) and rate equations can be determined using purified enzymes. Due to the high ATPase activity in the cell extract, determination of the GS and TryS activities was performed using a stepwise and end-point assay. For each enzyme, two separate reactions were prepared, one containing the three substrates and another lacking one of the specific substrates; the latter reaction accounted for the spurious ADP generated by ATPase activities (see Experimental procedures). The number of nmoles of ADP attributable to GS and TryS activities in cytosolic parasite extracts was approximately 6–12% of the total ATPase activity measured in the complete reaction. Nevertheless, a linear dependency of the ADP produced by GS and TryS activities on the amount of protein extract used was observed (Table S2); in contrast, the number of nmoles of ADP produced by ATPase background activity increased by only 25–33% when the amount of protein added was doubled. These

differences clearly show that only GS and TryS specific activities (but not ATPase activity) can be reliably determined under initial velocity conditions (linearity on the amount of protein used and saturating concentrations of the substrates). Moreover, the GS activities shown in Table 1 and Table S3 are well within the range reported for cell extracts from various organisms such as the parasites *Plasmodium berghei* (7.6 mU·mg protein⁻¹ [27]) and *Setaria cervi* (11 mU·mg protein⁻¹ [28]), the rat cell lines M22 and OC/CDE22 (3.9–7.8 mU·mg protein⁻¹) and rat kidney (39 mU·mg protein⁻¹) [29] using different experimental procedures. However, γ ECS activity could not be determined, most probably due to its scarcity in *T. cruzi* and other biological systems; indeed, γ ECS activities as low as < 2 mU·mg protein⁻¹ for plants [30] and 0.8–4 mU·mg protein⁻¹ for human and rat cells [29] have been reported.

On the other hand, TryR activity in cytosolic parasite extracts was determined with high reliability due to the natural high abundance of the enzyme and the high specificity of the spectrophotometric assay (Table 1). TXN and combined TXN-dependent peroxidase activities (TXNPx and nsGPxA activities) were also abundant in the parasites (Table 1). Moreover, no significant differences in the activities of GS, TryS and TryR were found between stressed and unstressed parasites and between 0 and 10 min of incubation (Table S3), indicating that a steady-state metabolic condition with no changes in enzyme activities had been attained in our experimental setting, a requirement for MCA experiments.

The V_{\max} values in the parasites indicated that GS and TryS activities (and probably γ ECS) were two orders of magnitude lower than those of TryR and the TXN-dependent antioxidant machinery (Table 1). However, a more appropriate comparison among enzymes involves consideration of the catalytic efficiency ($V_{\max}/K_{m,\text{thiol}}$). TryS and γ ECS showed the lowest efficiencies, suggesting that these enzymes may limit the flux under *in vivo* conditions (Table 1). Although the Spd concentration under control conditions was close to the TryS $K_{m,\text{Spd}}$, it decreased after the parasites were stressed (Table 2); thus TryS activity may be limited by two of its substrates.

The metabolite concentrations were determined under the three experimental conditions (Table 2). It is worth noting that some stress is generated just by subjecting the parasites to incubation, accounting for the observed changes in the T(SH)₂ and Spd concentrations (Table 2, columns 2 and 4). In this regard, Spd has been found to be oxidized under many types of stresses, including oxidative stress [31,32]. To diminish

this basal stress, other incubation media were tested, but similar patterns of response were obtained (data not shown). Despite this, significant additional oxidative stress was induced by adding peroxide, as indicated by the significantly diminished total GSH content as well as the decreased $T(SH)_2/TS_2$ ratios (from 15 to 7 after 10 min of incubation; Table 2, columns 4 and 6). Excretion of GSSG under oxidative stress conditions resulting in a loss of total GSH content has been reported previously for antimony-sensitive *Leishmania* [33], *Neurospora crassa* [34] and erythrocytes [35]. However, due to limitations in thiol measurement protocols, these oxidized compounds were not detected in the incubation medium of the epimastigotes.

The thiol compound contents in trypanosomatids are highly variable and depend on the strains and culture media used; however, our data for GSH and $T(SH)_2$ fall within the range reported for trypanosomatids [7], other *T. cruzi* strains, and for the strain used here cultured in two different media (Table S4). The Glu, Gly, γEC and ATP concentrations remained constant and saturating for the enzymes under the three conditions. The $NADP^+$ concentration did not change significantly (Table 2).

$T(SH)_2$ synthesis flux under the control condition was low, and increased two-fold in *T. cruzi* epimastigotes subjected to oxidative stress (Table 2, columns 4 and 6). The low flux to $T(SH)_2$ synthesis is related to the low activities and catalytic efficiencies in the synthetic pathway module (Table 1).

Kinetic model properties

The kinetic model for $T(SH)_2$ metabolism in *T. cruzi* was constructed using the metabolic simulator GEPASI/COPASI [36,37] (<http://www.copasi.org>) using the affinity constants for ligands of the recombinant pathway enzymes determined here under near-physiological conditions of pH and temperature (Table 1), and the V_{max} activities and precursor metabolite concentrations determined in the parasites under steady-state conditions (Tables 1 and 2). The reactions included in the model are shown in Fig. 4, and the model main features are described below. Details on its construction and rate-equation descriptions for each reaction are given in Experimental procedures and in Tables S5–S7.

All the reactions (except for the Spd, GSH and TS_2 leaks, which function as sinks) were considered reversible, including γECS , GS and TryS. The high K_{eq} values for the latter three were included in their rate equations to meet the thermodynamic constraints

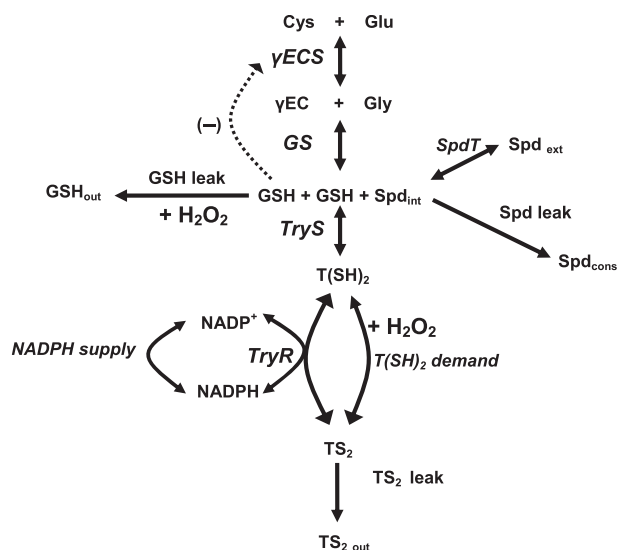


Fig. 4. Kinetic reactions of the model of *T. cruzi* $T(SH)_2$ metabolism. The model included enzymes for the synthesis of GSH and Spd transport (SpdT), the synthesis of $T(SH)_2$, the $T(SH)_2$ demand (oxidative stress plus the TXN-dependent peroxide detoxification system), the GSH, Spd and TS_2 leaks, the regenerating system (TryR) and the NADPH supply. As indicated, the reactions were considered reversible except for the GSH, Spd and TS_2 leaks; feedback inhibition of γECS by GSH was also included.

imposed by ATP hydrolysis on reaction reversibility. The reversibility of the reaction steps is a necessary condition to attain a stable steady state during kinetic model predictions; it allows the transfer of information throughout all the pathway components [38]. In addition, Spd was considered to be supplied only from the extracellular environment through the polyamine transporter(s), while its synthesis from *S*-adenosylmethione and putrescine (Put) (Fig. 1) was not included, because the contribution of the latter route to the Spd pool has been not studied. The supply of NADPH (derived from the oxidative section of the pentose phosphate pathway or by transhydrogenation) was also included to maintain the balance in the pyridine nucleotide concentration. In addition, H_2O_2 was included as a substrate of the $T(SH)_2$ demand reactions and GSH leak reactions in order to simulate stress and non-stress oxidizing conditions.

It has been previously demonstrated by MCA that the reactions that consume a pathway end-product (demand) significantly contribute to the control of flux and intermediary concentrations; for example, ATP demand for glycolysis in *Lactococcus lactis* and *Escherichia coli* [18] and GSH demand for GSH synthesis [39] (for details on supply/demand theory in MCA, see [40]). On the other hand, it has been observed that the peroxide detoxification system is abundant in

trypanosomatids [7–9]; TXN accounts for up to 3% (0.3–0.5 mM) of the total soluble protein content in *T. cruzi*, and TryR reaches 1.25 μM [41,42]; furthermore, 6% of the soluble protein in *C. fasciculata* corresponds to 2-Cys-Prx (TXNPx). The TXN-dependent peroxidase activities (corresponding to nsGPxA and TXNPx in Fig. 1) and TXN level determined in the epimastigotes used in this work were high (Table 1). These data indicate that the peroxide detoxification system has catalytic over-capacity compared with the T(SH)₂ synthetic pathway module; therefore, T(SH)₂-demanding processes, i.e. oxidative stress and the antioxidant machinery (TXN, TXNPx and nsGPxA), were combined into a single reversible reaction (T(SH)₂ demand).

Due to the decrease of the total contents of Spd, GSH and T(SH)₂ under oxidative stress conditions (the latter two most probably in oxidized form; Table 2), it was necessary to include reactions representing leaks for those metabolites; in their absence, the model did not accurately predict the intermediary concentrations found under oxidative stress conditions. The cellular mechanisms involved in these phenomena are highly interesting but beyond the scope of this study.

Using the model, three conditions were analyzed: (a) basal non-incubated parasites, (b) parasites incubated in the absence of H₂O₂, or (c) parasites incubated in the presence of 20 μM H₂O₂. The model predictions displayed hyperbolic patterns, indicating that under all tested conditions a stable steady state was reached.

Validity and robustness of the kinetic model

Construction and validation of kinetic models are performed using different datasets. For construction, datasets for the individual enzymes were used (affinity constants for ligands and V_{max} in cells), and, for validation, datasets obtained from the complete system (i.e. intermediary concentrations and pathway fluxes measured *in vivo*) were compared with model-predicted datasets. Hence, a validated kinetic model is one that can accurately predict pathway behaviour within the biological variability of the *in vivo* parameters [19,20,43].

Under the three modelled conditions, the concentrations of the thiol molecules Spd and NADP⁺ were within 0.36–1.85 times the average concentrations determined *in vivo* (Table 2; columns 3, 5 and 7). The predicted flux agreed with that measured *in vivo* under control conditions; however, the predicted flux under stress was 0.3 times the experimental value (Table 2). This variation was due to inclusion of the highly H₂O₂ concentration-sensitive GSH leak reaction; however, in its absence, a fourfold higher GSH concentration was

predicted compared to the experimental value. To further explore these interactions, the T(SH)₂ synthesis flux and thiol concentrations were modelled at different rates of GSH and T(SH)₂ leaks (Fig. S4). A higher dependency on the GSH leak rate was observed, correlating with the observed diminution in GSH levels in the parasites in the presence of the oxidant (Table 2). For the basal condition, the rate constant (k) values for T(SH)₂ demand and the GSH and Spd leaks were modified to obtain the higher Spd concentration observed in the *in silico* experiment; these changes avoided GSH and T(SH)₂ accumulation. Overall, the kinetic model closely predicted the metabolite steady-state concentrations and fluxes in the parasites under each experimental condition.

The kinetic model also showed high robustness (Table S8); it permitted decreases or increases in the values of the affinity constants and V_{max} values of the enzymes without significantly altering the pathway control distribution, i.e. the steps that exerted the greatest control remained the same. Flux control was redistributed between γECS and TryS when their V_{max} values or the $K_{\text{m,Cys}}$ for γECS and the $K_{\text{m,Spd}}$ for TryS (Table S8) were varied by 50%. Only when the V_{max} values were decreased was the flux significantly decreased. As expected, variation of the TryR V_{max} only modified the T(SH)₂ concentration (< 50%) and the T(SH)₂/TS₂ ratio, but not the TS₂ concentration, because the latter is controlled by oxidative stress (Table S8). Remarkably, decrease of γECS and TryS activities by 50% resulted in a decreased TS₂ concentration. The model was not sufficiently robust to accurately predict the pathway behaviour at > 20 μM H₂O₂, because, at this concentration, the T(SH)₂ demand reaction completely depleted the T(SH)₂ concentration. However, at 10 μM H₂O₂, the model predicted highly similar metabolite concentrations and fluxes to those experimentally determined in parasites incubated with 50 μM H₂O₂, suggesting that, *in vivo*, the parasites were perhaps exposed to 10 μM H₂O₂, and that the rest of the added H₂O₂ reacted with the incubation medium.

Control structure of T(SH)₂ metabolism in *T. cruzi*

Flux control distribution

The kinetic model provided the flux control coefficients for each reaction step under the three experimentally evaluated conditions (Table 3). Under basal conditions (which reflect the culture conditions as the parasites were analysed shortly after harvest), the main flux control step was γECS , with a low but significant contribution of TryS. The rest of the pathway steps did not contribute to flux control.

Table 3. Control coefficients of the T(SH)₂ synthesis enzymes. The pathway flux was considered to be through the TryS reaction. The negative sign for the flux control coefficients for some steps indicates that their activities do not favour T(SH)₂ synthesis flux because they either consume precursors for its synthesis or regenerate the metabolite.

Condition	Basal	Control	Stress
Enzyme/process (<i>ai</i>)	C_{ai}^J		
γ ECS	0.84	0.58	0.7
GS	0.0011	6.5×10^{-4}	9.8×10^{-4}
TryS	0.14	0.49	0.58
SpdT	0.016	0.24	0.22
TryR	-0.0029	-0.012	-0.0095
T(SH) ₂ demand	0.003	0.012	0.0095
NADPH supply	-3×10^{-5}	-1.6×10^{-4}	-5.5×10^{-5}
Spd leak	-1.5×10^{-4}	-0.17	-0.17
GSH leak	-8.2×10^{-5}	-0.14	-0.35
TS ₂ leak	1.5×10^{-4}	7.7×10^{-4}	6.9×10^{-4}

Under unstressed control conditions, a 31% decrease in $C_{\gamma ECS}^J$ was observed whereas TryS flux control significantly increased, in parallel with increased flux control by Spd supply and the Spd and GSH leaks (Table 3). The augmented flux control by TryS is a consequence of the sixfold decrease in Spd content seen under control and stress conditions (Table 2), such that it becomes non-saturating for the enzyme; in addition, the decrease in Spd also resulted in increased control by its supply and demand reactions. The model predicted a similar flux control distribution in the stressed parasites (Table 3); the increased flux control by γ ECS and TryS was proportional to the increase in flux control by the GSH leak, which accounted for the large decrease in GSH concentration under these conditions (Table 2). TryR did not exhibit significant control of T(SH)₂ synthesis flux under any of the three modelled conditions. Unexpectedly, the T(SH)₂ demand also exhibited low control of the T(SH)₂ synthesis flux.

Remarkably, the model-predicted T(SH)₂ synthesis fluxes of 0.5–0.9 nmol·min⁻¹·mg protein⁻¹ contrasted with the high fluxes through the TryR/T(SH)₂ demand/NADPH supply pathway module of approximately 248 nmol·min⁻¹·mg protein⁻¹ (Table 2). Hence, kinetic modelling indicated a bi-functional modular organization of T(SH)₂ metabolism in the parasite.

Why do γ ECS and TryS control the synthesis of T(SH)₂?

The elasticity coefficients of the pathway enzymes and transporters help to establish the molecular mechanisms

that explain why an enzyme controls, or does not control, the pathway flux. The elasticity coefficient (ε_X^{ai}) represents the change in the rate or activity (*a*) of a pathway enzyme/transporter (*i*) relative to the change in the concentrations of its ligands *X* (substrates, products or modulators). The elasticity coefficients are intrinsic properties of the enzymes (in contrast to flux and concentration control coefficients, which are systemic properties), and are only determined by the particular kinetic features of each enzyme [17,18]. Moreover, the elasticity coefficients are inversely related to their flux control coefficient: the rate of an enzyme with low elasticity (ε_X^{ai} approaching to 0) cannot increase at increasing substrate concentrations, representing a constraint in the pathway flux [17,18].

γ ECS is competitively inhibited by GSH versus Glu, and has the lowest elasticity coefficient for the thiol molecule amongst the pathway enzymes (Table S9). To determine whether the γ ECS high flux control was due to low enzyme activity in the parasites or to GSH feedback inhibition at physiological concentrations of its ligands (Glu and γ EC), the pathway was modelled under a wide range of $K_{i,GSH}$ values (0.1–10 times the experimentally determined value), resulting in no changes in the control distribution (data not shown). As the Glu and GSH intracellular concentrations are 5.6- and 0.5 times the K_m and K_i values, respectively, the contribution of GSH feedback inhibition to the high γ ECS flux control appears to be negligible. TryS showed high elasticity for its substrates (Table S9); thus, its high control can only be explained by its low activity in the cells. Within this T(SH)₂ synthesis module, GS exhibited the highest elasticity towards the thiol ligand, such that this enzyme exerted the lowest control (Table S9). TryR had a low elasticity coefficient for TS₂, but the presence of high activity in the cell resulted in negligible flux control. In conclusion, the high flux control of the T(SH)₂ synthesis enzymes is mainly derived from their low activities in these parasites.

Concentration control distribution

In contrast to control of the pathway flux, control of T(SH)₂ concentration was exerted by its demand and TryR under the three modelled conditions (Table 4). To visualize whether the synthetic pathway contributes to T(SH)₂ concentration control, a model was constructed from which TryR was not included (data not shown). Using this truncated model, the values for the control coefficients of the T(SH)₂ concentration were similar to the flux control coefficients for γ ECS, TryS, spermidine transport (SpdT) and the Spd leak

Table 4. Control coefficients on the T(SH)₂ concentration of the pathway enzymes. Negative coefficients indicate that these reactions either consume T(SH)₂ or consume a precursors.

Condition	Basal	Control	Stress
Enzyme/process (<i>ai</i>)	$C^{[T(SH)_2]}_{ai}$		
γECS	0.04	0.038	0.053
GS	5.7×10^{-5}	4.2×10^{-5}	7.25×10^{-5}
TryS	0.007	0.03	0.04
SpdT	8.8×10^{-4}	0.015	0.016
TryR	0.98	0.97	0.99
T(SH) ₂ demand	-0.99	-0.99	-0.99
NADPH supply	0.01	0.013	0.0058
Spd leak	-7.9×10^{-6}	-0.01	-0.013
GSH leak	-4.4×10^{-6}	-0.009	-0.026
TS ₂ leak	-0.05	-0.062	-0.072

(Table 3), except for T(SH)₂ demand, whose control coefficient value remained -0.99.

Kinetic modelling for drug target identification in the T(SH)₂ metabolism of parasites

According to the fundamental principles of MCA, in order to inhibit the flux of a hypothetical linear pathway by 50%, an equal percentage inhibition must be attained for a pathway enzyme that has a flux control coefficient equal to 1 (a true rate-limiting step) [17,18]. Due to the branched nature of metabolic pathways and the shared control of metabolic fluxes, higher percentage inhibition is usually necessary for enzymes with lower control coefficients, and almost complete inhibition is necessary for enzymes with insignificant control.

The kinetic model described above predicted that, to inhibit the flux of T(SH)₂ synthesis by 50%, it is necessary to inhibit the individual activities of γECS, TryS and SpdT by 58, 63 and 73%, respectively (Fig. 5A). Furthermore, combined 50% inhibition of the first two enzymes or 40% inhibition of the three proteins resulted in the same decrease in flux. In marked contrast, 99% inhibition of TryR did not affect the synthesis of T(SH)₂ (Fig. 5A), as expected from its low flux control coefficient. On the other hand, due to the high TryR control coefficient on the concentration of reduced T(SH)₂, the kinetic model predicted that TryR inhibition causes a linear decrease in the metabolite level (Fig. 5B). However, the T(SH)₂ concentration is also remarkably affected by the activities of γECS, TryS or SpdT when they are inhibited by > 70% (Fig. 5B).

The model also predicted that, to decrease the T(SH)₂ reductive capacity of the parasites by 50%,

60% increased oxidative stress (T(SH)₂ demand) combined with a 25% decrease in TryR activity was required (Fig. 5C). With no TryR inhibition, a more than twofold increase in T(SH)₂ demand (Fig. 5C), or alternatively 50–75% inhibition of γECS (Fig. 5D), was necessary to achieve a similar decrease in T(SH)₂ reductive capacity. On the other hand, the decrease in T(SH)₂ synthesis flux brought about by inhibiting γECS and TryS was not further potentiated by increasing oxidative stress (Fig. 5E,F).

Discussion

Characteristics of T(SH)₂ metabolism pathway enzymes, metabolite concentrations and fluxes

The kinetic constants of the recombinant purified pathway enzymes were determined under near-physiological conditions of temperature and intracellular pH. The kinetic properties of GS from *T. cruzi* are reported for the first time for a trypanosomatid species, thus completing characterization of the GSH synthetic pathway in these parasites. The kinetic parameters of the recombinant enzymes were similar to those previously reported in the literature (Table S1), except for the lack of GSH inhibition of recombinant and native TryS. Notably, the affinity of TryS from *T. cruzi* strains for GSH is one order of magnitude lower than that for the enzymes from *T. brucei* and *Leishmania* (Table S1).

The V_{\max} of most of the pathway enzymes was determined here in *T. cruzi* epimastigotes, except for γECS. These values are critical for construction of the kinetic model as they reflect the amount of active enzyme inside living cells. Estimation of the *in vivo* V_{\max} from the content of protein determined by western blot was avoided because, in our experience, there is no linear correlation between the content of protein and the amount of active enzyme [44–46], resulting in miscalculated control coefficients.

Comparison of the catalytic efficiencies V_{\max}/K_m of the pathway enzymes suggested that $\gamma\text{ECS} \geq \text{TryS} \gg \text{GS}$, in the precursor supply module, limit T(SH)₂ *de novo* synthesis in the parasites. In contrast, TryR and the TXN-dependent antioxidant machinery (TXN, TXNPx and GPXA), in the T(SH)₂-consuming module, have over-capacity (high catalytic efficiency *in vitro* and *in vivo*, and saturation for the substrates). The low catalytic efficiencies of the enzymes of the T(SH)₂ supply module correlated with the low pathway fluxes determined *in vivo* (Table 2). Therefore, the most probable reason why TryR and the TXN-dependent peroxide detoxification system are abundant in

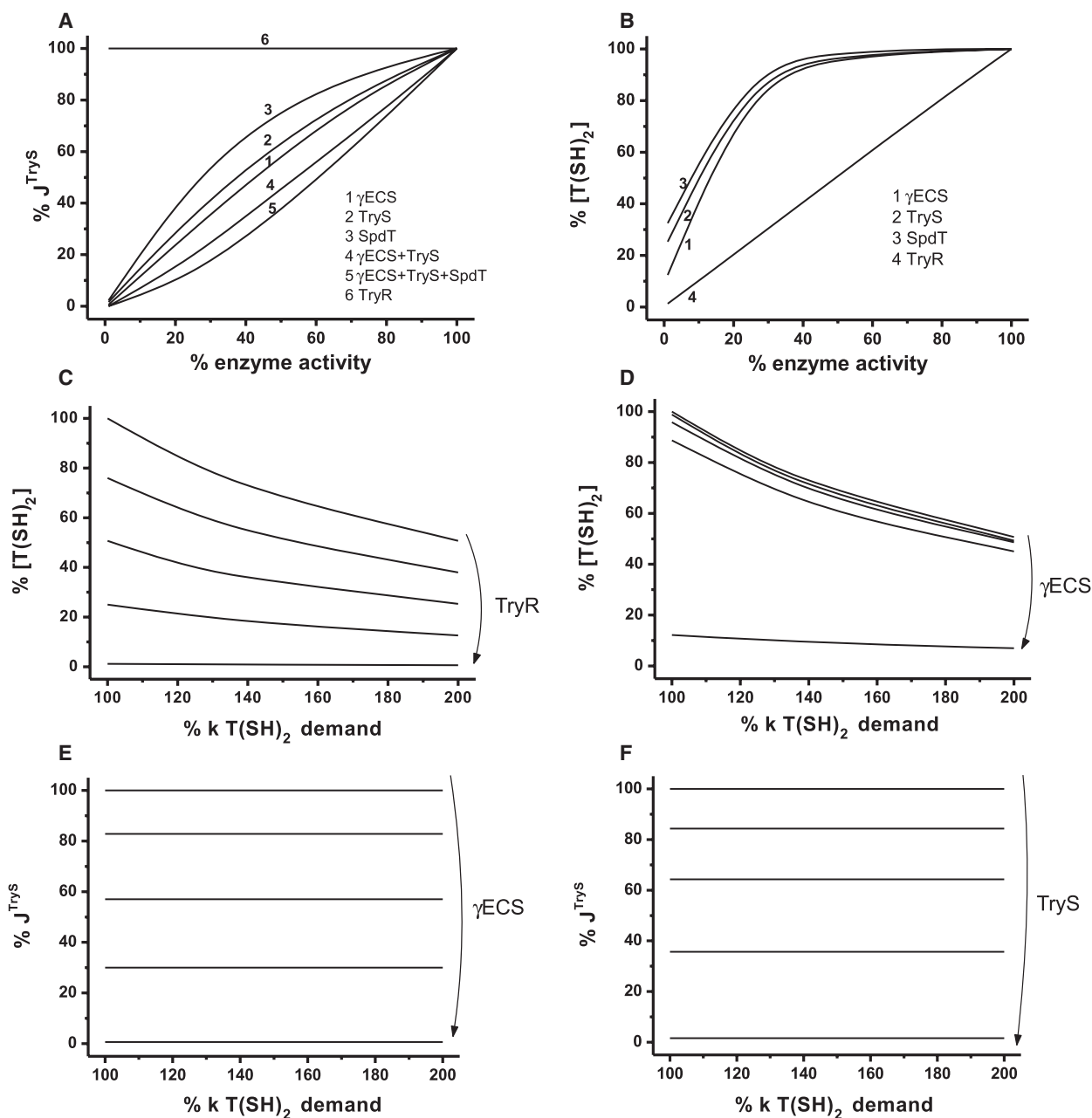


Fig. 5. Predictions using the kinetic model under control conditions. (A) Effect of decreasing the activity of γ ECS, TryS, SpdT, TryR, and combinations thereof on the flux through TryS. Inhibition of the three steps that exert the greatest control affects the flux almost linearly, whereas TryR has no effect. (B) Effect of decreased γ ECS, TryS, SpdT and TryR activity on T(SH)₂ concentration. TryR inhibition affects the metabolite concentration linearly, whereas γ ECS, TryS and SpdT have to be inhibited by > 70% to decrease the metabolite concentration. (C) Effect of increasing the T(SH)₂ demand rate at various TryR activities. Simultaneous inhibition of TryR and increasing the demand module lead to synergistic T(SH)₂ depletion. (D) Effect of increasing the T(SH)₂ demand module at various concentrations of γ ECS. Due to the low control that γ ECS exerts on the T(SH)₂ concentration, the synergistic effect is important until γ ECS is inhibited by > 75%. (E,F) Increasing the rate of T(SH)₂ demand has no synergistic inhibitory effect on the T(SH)₂ concentration when combined with inhibition of γ ECS and TryS. For (C–F), the activities indicated on the right were modulated at 100, 75, 50, 25 and 1% of their original V_{max} values. Note that 100% activity is different for each enzyme, being two orders of magnitude higher for TryR. Thus, the potency and specificity of the inhibitors must be higher for TryR than for γ ECS and TryS.

the parasites is to provide an efficient system to immediately deal with external perturbations that decrease the $T(SH)_2/TS_2$ ratio, before activation of the much slower *de novo* $T(SH)_2$ synthesis pathway under prolonged periods of oxidative stress.

Kinetic modelling of $T(SH)_2$ metabolism

Kinetic models of metabolic pathways in human parasites have been described only for glycolysis in *T. brucei* [47] and *Entamoeba histolytica* [48,49] and the glyoxalase system in *Leishmania infantum* [50]. The first kinetic model of $T(SH)_2$ metabolism in a trypanosomatid reported here facilitates understanding of the controlling mechanisms of this important pathway in these parasites.

The kinetic model predicted that $T(SH)_2$ synthesis was mainly controlled (50–70%) by γ ECS and TryS (Table 1), as a result of their relatively low cellular active contents and non-saturating thiol and polyamine substrates (Table S9). The negligible contribution of feedback inhibition by GSH to the high flux control coefficient of γ ECS was a consequence of the high $[Glu]/K_{m,Glu}$ ratio of 59–69 and low $[GSH]/K_{i,GSH}$ ratio of 0.25–0.5: the competing substrate predominantly binds the enzyme and blocks inhibitor binding. These results emphasize the need to abandon the dogmatic concepts of a ‘rate-limiting step’ or an ‘allosteric or feedback-inhibited enzyme’ as the only criteria to describe the controlling steps of metabolic pathways [13,17,18,46]. In contrast, an integral and dynamic network analysis of the pathway can allow precise and quantitative predictions regarding the relevance of a particular enzyme for control of the metabolic pathway, and may unveil unknown interactions among enzymes and metabolites.

The enzymes/processes that control the concentration of $T(SH)_2$ were mainly its demand (oxidative stress) and TryR. However, γ ECS and TryS also exert control when they are strongly inhibited or when TryR is absent or inhibited. An explanation for this behaviour is that TryR serves as a buffer enzyme to maintain a constant $T(SH)_2/TS_2$ ratio; however, the total $T(SH)_2$ concentration in the cell will only depend on the flux through the synthetic module. Thus, γ ECS and TryS may potentially exert significant control on the total $T(SH)_2$ concentration in these parasites. In various drug-resistant *Leishmania* strains, an increased content of the enzymes of the $T(SH)_2$ synthesis and antioxidant machinery was determined by microarrays and western blot analyses [51–54]. This indicates that enhancement of $T(SH)_2$ synthetic enzymes is also required to potentiate the antioxidant capabilities of the parasites.

Metabolic modelling also allows the identification of emergent properties of the network that cannot be identified by studying its elements in isolation or as separate pathways [15]. In this regard, the kinetic model identified $T(SH)_2$ metabolism as comprising a catalytically slow and less efficient synthetic module (γ ECS, GS, TryS and SpdT) and a fast and highly efficient module (the antioxidant enzymatic machinery and TryR), connected through the common metabolite $T(SH)_2$. Moreover, it indicated that excretion of oxidized thiols under oxidative stress may also have a significant effect on the antioxidant capabilities of the parasites as a result of loss of essential GSSG and TS_2 (oxidized) moieties. These pathway emergent properties were only recognized by studying the enzymes and transporters in the network.

It is worth emphasizing that the present *T. cruzi* epimastigotes-based kinetic model may be used as a core model to which the particular variations of the pathway between parasite stages or different trypanosomatid species can be added once metabolomic and enzymatic (kinetomic) data become available. For example, the polyamine synthetic pathway lead by *S*-adenosyl methionine decarboxylase and ornithine decarboxylase in *T. brucei* and *Leishmania*, Spd enzymatic synthesis in *T. cruzi* (Fig. 1), and the oxidative section of the pentose phosphate pathway, which provides NADPH for the antioxidant machinery, are pathways that are directly connected to the reactions considered in the present kinetic model. Another useful application of kinetic/mathematical models is the readiness to predict possible pathway scenarios under different physiological conditions. As discussed above, the most critical parameter for kinetic modelling is the V_{max} value determined in cells; obtaining this parameter for the steps identified here as exerting the greatest control, and measurements of relevant metabolites (GSH, $T(SH)_2$ and Spd) and pathway fluxes in the human stages of *T. cruzi*, may extend the benefits of the present kinetic model. Moreover, the robustness of the model and pathway permits the hypothesis that the steps that exert the greatest control will probably be the enzymes with the lowest activities in cells of *T. cruzi* trypanomastigotes and amastigotes.

Utility of kinetic modelling for drug target validation

Kinetic modelling is a useful systems biology approach that facilitates the identification of drug targets with the highest therapeutic potential. Thus, drug design focusing on the steps that exert the greatest control in the network for multi-target inhibition emerges as a

substantiated sound and novel strategy that contrasts with the traditional approach of attempting to fully inhibit non-controlling steps or the 'rate-limiting' steps reported in biochemistry textbooks [13]. Many metabolic enzymes from parasites display substantial differences regarding their allosteric modulation compared to their human counterparts [47–49,55,56], and these differences may be exploited for species-specific targeted therapy. For these reasons, it is worthwhile to embark on a complete kinetic description of parasite enzymes and study them using network-based analysis for validation as drug targets.

Based on the model predictions (Fig. 5), we propose that simultaneous inhibition of the flux-controlling enzyme γ ECS and TryS will have more striking effects on T(SH)₂ metabolism than separate inhibition. Thus, use of combination therapies, or design of multi-target drugs for these enzymes, are interesting starting points for alternative chemotherapy against *T. cruzi* and possibly other trypanosomatids. However, the possible presence of GSH transporters in *T. cruzi*, as suggested for *T. brucei* and *Leishmania* [57,58], may diminish the flux control of γ ECS and increase those of TryS and SpdT. Therefore, more studies are required on GSH transport in these parasites for a complete understanding of pathway control mechanisms.

With regard to multi-target therapy, it was previously reported that the parasitocidal effects of nifurtimox and benznidazole were increased by co-treatment with buthionine sulfoximine [59,60], an irreversible inhibitor of γ ECS that also appears to inhibit GSH transport in *T. brucei* [57]. By inhibiting *de novo* T(SH)₂ synthesis using buthionine sulfoximine and increasing oxidative stress using commercial drugs, a stronger inhibitory effect on trypanothione metabolism (and growth) was achieved, suggesting that pharmacological intervention on several reactions at lower doses, rather than inhibiting individual enzymes at higher doses, is a more efficient approach to affect the pathway.

Because TryS is not present in the host and has a high flux control coefficient in the pathway, it appears to be the most relevant drug target in T(SH)₂ metabolism. Recently, potent non-competitive inhibitors (in the nanomolar range) against purified TryS from *T. brucei* were identified by high-throughput screening of a chemical compound library; however, their effects on growth and thiol contents were achieved in the micromolar range [61], indicating how cellular complexity can make successful drug discovery difficult [62].

On the other hand, TryR inhibition, together with oxidative stress, may favour an oxidized cellular state

only when the T(SH)₂ synthesis pathway is not activated. Inhibition of TryR or the antioxidant machinery enzymes for therapeutic purposes will be a very challenging task because their high activity in the cell will require the design of highly specific and potent inhibitors or use of high concentrations, with probable severe side-effects for patients. Therefore, inhibition of already limiting enzymes such as γ ECS and TryS is therapeutically more promising than inhibition of abundant enzymes such as TryR or the peroxide detoxification machinery.

Correlations of the kinetic model predictions with experimental genetic results in other trypanosomatids

The results yielded by kinetic modelling indicated that γ ECS and TryS were the main controlling steps of T(SH)₂ synthesis flux, and probably also of the total T(SH)₂ concentration under prolonged stress conditions. Decreased expression (50–80%) of γ ECS induced by genetic means in *T. brucei* and *Leishmania* resulted in almost 50% decreased content of GSH and T(SH)₂ [57,58]. Moreover, treatment of *T. cruzi* with buthionine sulfoximine decreased the intracellular thiol content by 70–80% [59,60]. These results are in agreement with predictions by the present kinetic model regarding the high control that this enzyme exerts on the pathway.

TryS down-regulation in *T. brucei* (85%) promotes fourfold accumulation of GSH and a 10% increase in the amount of Spd, respectively, in addition to an 86% decrease in T(SH)₂ levels [63,64] versus control parasites, in agreement with the predictions of the model (Fig. 5B). Although TryS down-regulation also induced an increase in γ ECS and TryR activities *in vivo*, most probably to compensate for T(SH)₂ depletion, parasite resistance to oxidative stress was impaired and cellular viability was compromised.

SpdT, as the main supply of Spd, showed lower control of T(SH)₂ synthesis compared to γ ECS and TryS, due to its higher catalytic efficiency ($V_{\max} = 5.8 \text{ nmol}\cdot\text{min}^{-1}\cdot\text{mg cell protein}^{-1}$; $K_{\text{m,SpdT}} = 0.81 \text{ }\mu\text{M}$) [65]. The molecular identity and kinetic characterization of an Spd transporter in *T. cruzi* has been reported ($V_{\max} 3.6 \text{ pmol}\cdot\text{min}^{-1}$ per 10^7 cells, i.e. approximately $156 \text{ pmol}\cdot\text{min}^{-1}\cdot\text{mg cell protein}^{-1}$; $K_{\text{m}} 0.014 \text{ mM}$) [66]. By using these other kinetic parameters, full control by SpdT was achieved because of the extremely low catalytic efficiency (data not shown). Thus, further studies on Spd uptake kinetics are necessary. On the other hand, fast high-affinity transporters for Put/cadaverine have been well characterized in *T. cruzi*

epimastigotes [65–68]. Unfortunately, there is limited information regarding the rate of Spd synthesis from Put (Fig. 1), although it appears to be fast [69]; spermidine synthase (SpdS) from *T. cruzi* has not been characterized. This additional internal source of Spd may further decrease the control exerted by SpdT. Furthermore, *de novo* Spd synthesis from ornithine is possible in *T. brucei* and *Leishmania* [9,70]; hence, redistribution of the control coefficients is expected in these trypanosomatids.

TryR showed negligible control on the synthesis of T(SH)₂. In agreement with its predicted control properties, knocking down TryR in both *T. brucei* (< 10% remaining activity) and *Leishmania* did not modify the total thiol content [71,72].

Using the present kinetic model to reproduce longer oxidative stress conditions under which enzyme activities change will require re-determination of fewer experimental parameters than determined in this work, i.e. V_{\max} , thiol contents, and fluxes under the new steady state.

Concluding remarks

From the perspective of the organization of intermediary metabolism, all constituent enzymes and transporters are essential for proper pathway function, because deleting any of them creates a gap in the pathway flux. However, from the perspective of the control of metabolism, not all of the pathway components have therapeutic potential, only those that exert significant pathway control. Genetic strategies can determine whether a pathway component is essential for cell function. Kinetic modelling predicts how essential each pathway component is by determining their control coefficients. Hence, kinetic modelling of T(SH)₂ metabolism in parasites assists in validation of drug targets with the highest therapeutic potential by identifying the enzymes with the highest control on the pathway flux and T(SH)₂ concentration (i.e. $\gamma\text{ECS} \geq \text{TryS} \gg \text{SpdT}$).

Experimental procedures

Reagents

ATP, γEC , trifluoroacetic acid, 5,5'-dithio-bis(2-nitrobenzoic acid), haemin, imidazole, sodium borohydride (NaBH₄), MES, potassium phosphate monobasic, trehalose, catalase, GSH, MgCl₂, EDTA, dansyl chloride, methanol, diethylenetriamine pentaacetic acid, *N*-ethylmaleimide and NADH were purchased from Sigma (St Louis, MO, USA); glycine, MOPS, dithiothreitol and Hepes were purchased from Research Organics (Cleveland, OH, USA); acetonitrile and

NaCl were purchased from Caledon (Georgetown, Ontario, Canada); triethanolamine, perchloric acid, sodium phosphate dibasic and glucose were purchased from JT Baker (Phillipsburg, NJ, USA); phosphoenolpyruvate and β -mercaptoethanol were purchased from ICN Biomedicals (Aurora, OH, USA); H₂O₂ was purchased from Laboratorios American (Mexico City, Mexico); isopropyl- β -D-thiogalactoside was purchased from Amresco (Solon, OH, USA); Tris was purchased from IBI Scientific (Peosta, IA, USA).

Culture conditions

Epimastigotes of *T. cruzi* Querétaro strain (TBAR/MX/0000/Querétaro) [21] were cultured in RPMI-1640 medium (Sigma) supplemented with 10% fetal bovine serum (PAA Laboratories, Pasching, Austria). The cultures were incubated at 26 °C as described previously [73]. Parasite cultures were started in 20 mL medium and scaled up, always maintaining a density of 2×10^6 parasites per mL, to reach 500 mL after 6 days, then harvested. For TXN and TXN-dependent peroxidase activities, the parasites were cultured in liver infusion tryptose medium (DIFCO, Detroit, MI, USA), supplemented with 10% fetal bovine serum and 25 $\mu\text{g}\cdot\text{mL}^{-1}$ haemin, and maintained at 26 °C. In this case, parasite cultures were initiated at a density of 4×10^6 parasites per mL and harvested after 5 days, reaching a density of approximately 25×10^6 parasites per mL.

Gene amplification

Genomic DNA from the *T. cruzi* Ninoa strain was isolated as previously described [74]. γECS , GS, TryS, TryR, TXN, nsGPxA and TXNPx genes were amplified by PCR using genomic DNA from this strain. The nucleotide sequences of the primers used for each gene are: γECS (sense 5'-CGT ACCATGGGTCTCTTGACAACG-3', antisense 5'-TAG CCTCGAGCTCACGGGATCTTTTGG-3'); GS (sense 5'-CGTACATATGGAAGCTTTGGGGGAC-3', antisense 5'-TAGCGTTCGACTTAAACAAGCGCCAGTGA-3'); TryS (sense 5'-CGTACCATGGGCTCTTTGGCGGTACCA-3', antisense 5'-TAGCAAGCTTCGTTTTCAAGCCACC-3'); TryR (sense 5'-CGTACATATGATGTCAAAGATTTT TG-3', antisense 5'-TAGCAAGCTTTTACAGAGATGCTT CTGA-3'); TXN (sense 5'-CGTACATATGTCTGGTTTG GCGAAGTAC-3', antisense 5'-GCTAAGCTTTTAGTCG GACCAGGGGAAG-3'); nsGPxA (sense 5'-GCACATAT GTTTCGTTTCGGTCAATTGCTTAG-3', antisense 5'-GC TAAGCTTTCAAATCCTAGCACCACCAAG-3'); TXNPx (sense 5'-CGTACATATGTCTGCGGAGACGC-3', antisense 5'-CGATAAGCTTCTACGCGGACAGCACC-3'). All sequences contain *Nde*I and *Hind*III restriction sites. The PCR products were cloned in the pGEM[®]-T Easy vector (Promega, Madison, WI, USA), and their identity was confirmed by nucleotide sequencing.

Over-expression and protein purification

The genes were cloned into the *NdeI* and *HindIII* restriction sites of the pET28 plasmid (Novagen, Darmstadt, Germany), which was used to transform *Escherichia coli* BL21(DE3) cells in order to over-express the proteins fused to a histidine tail. The cells were grown at 37 °C in Luria–Bertani medium to an attenuation at 600 nm of 0.6; then protein expression was induced by adding 0.4 mM isopropyl- β -D-thiogalactoside, and the cells were further cultured overnight at 25 °C. The cells were harvested and resuspended in 20 mL buffer containing 100 mM triethanolamine, pH 7.4, 300 mM NaCl and 2 mM imidazole, and lysed in a French press (AMINCO SLM, Rochester, NY, USA) by passing the cellular suspension three times at 20 000 psi (137.9 MPa) for TryS and TryR, four times at 20 000 psi for γ ECS, and four times at 16 000 psi (110.3 MPa) for GS. The protocol was optimized for each enzyme because they were highly susceptible to inactivation by sonication, high pressures and the number of passages. For analyses of TXN, GPxA and TXNPx, bacteria were lysed by sonication using a Branson Sonifier 450 (Emerson, Danbury, CT, USA) with one cycle of 30 s at 20% output, one cycle of 1 min at 10–15% output, and one cycle of 30 s at 20% output. Each cycle was followed by a 1 min incubation on ice. The bacterial lysates were centrifuged at 7818 g for 15 min at 4 °C. The enzymes were purified from the supernatant at room temperature by Co^{2+} -affinity chromatography using Talon resin (Clontech, Mountain View, CA, USA) as previously described [56]. The enzymes were concentrated at 0.5–2 mg·mL⁻¹ for γ ECS and TryS, 5 mg·mL⁻¹ for GS, 7–9 mg·mL⁻¹ for TryR, 19.3 mg·mL⁻¹ for TXN, 12.2 mg·mL⁻¹ for nsGPxA and 6 mg·mL⁻¹ for TXNPx. The enzymes were stored at -20 °C in the presence of 50% glycerol for TXN, nsGPxA, TXNPx and TryR. γ ECS, GS and TryS recombinant enzymes were relatively unstable under any storage conditions, such as 50% glycerol at -20 °C or 3.2 M ammonium sulfate at 4 °C; only the presence of 0.5 M trehalose for γ ECS and TryS and 1 M trehalose for GS and storage at 4 °C improved their stabilities.

Kinetic characterization

All the reactions and kinetic parameters were determined at 37 °C. The activities of recombinant γ ECS, GS and TryS were determined by coupling the ADP production to pyruvate kinase/lactate dehydrogenase (Roche, Mannheim, Germany) and following the NADH oxidation at 340 nm. The standard reaction mixture contained 40 mM Hepes/NaOH, pH 7.4, 5 mM MgCl₂, 1 mM EDTA, 1 mM phosphoenolpyruvate, 0.2 mM NADH, 2–2.8 units (micromol/min) pyruvate kinase/lactate dehydrogenase in ammonium sulfate, and 2–5 μ g enzyme plus specific substrates: for γ ECS, 1.3 mM Glu and 0.6 mM ATP, plus 2.1 mM Cys to

start the reaction; for GS, 8 mM Gly and 0.9 mM ATP, plus 0.4 mM γ EC to start the reaction; for TryS, 11 mM Spd and 0.7 mM ATP, plus 7.6 mM GSH to start the reaction. The K_m for each substrate was determined using saturating concentrations of the two co-substrates (as in the standard reactions). The concentrations of the substrates were varied as follow: for γ ECS, 0–2 mM Cys, 0–2 mM Glu and 0–1 mM ATP; for GS, 0–0.4 mM γ EC, 0–10 mM Gly and 0–1.5 mM ATP; for TryS, 0–5 mM GSH, 0–11 mM Spd and 0–1 mM ATP. TryS purified from bacteria disrupted by sonication showed hysteresis; however, by starting the reaction with Spd or by disrupting bacteria using the French press, this phenomenon was not observed (data not shown).

TryR activity was determined spectrophotometrically following NADPH oxidation at 340 nm. The standard reaction mixture contained 40 mM Hepes, pH 7.4, 1 mM EDTA, 0.07–0.09 μ g TryR, 0.24 mM TS₂ (Bachem, Torrance, CA, USA) and 0.2 mM NADPH. For K_m determinations, the NADPH concentration was varied from 0 to 0.2 mM (saturating with 0.24 mM TS₂) and the TS₂ concentration was varied from 0 to 0.4 mM (saturating with 0.2 mM NADPH).

For GS $K_{i,\text{GSH}}$ determination, saturation curves for each substrate were determined as described above (for the K_m determination) in the presence of varying GSH concentrations (0–10 mM). For γ ECS, $K_{i,\text{GSH}}$ and $K_{i,\gamma\text{EC}}$ saturation curves for Glu were determined in the presence of 0–3 mM γ EC or 0–5 mM GSH.

The effect of TS₂, GSSG and T(SH)₂ on the three enzymes was determined using saturating concentrations of their substrates. The concentrations tested were within the physiological range of concentrations.

The TXN, nsGPxA and TXNPx activities were determined by reconstituting the antioxidant pathway in the presence of TS₂ and TryR, and spectrophotometrically monitoring NADPH oxidation at 340 nm. In all cases, it was ensured that all added TS₂ was reduced by TryR before addition of the enzyme of interest. The 0.5 mL standard reaction mixture contained 40 mM Hepes, pH 7.4, 1 mM EDTA, 0.16 mM NADPH, 0.4 mM TS₂, and the following proteins and substrates: for TXN (0.12–0.16 μ M), 0.5 μ M TryR, 20 μ M TXNPx and 0.52 mM *tert*-butylhydroperoxide (t-butOOH); for nsGPxA (0.03–0.076 μ M), 0.5 μ M TryR, 22 μ M TXN and 1 mM cumene hydroperoxide (CumOOH); for TXNPx (1 μ M), 0.045 mM TS₂, 10 mM TryR, 1 μ M TXN and 120 μ M t-butOOH. The reactions were started by addition of the enzyme of interest at the indicated concentrations. The K_m for each substrate was determined by varying one of the substrates and using saturating concentrations of the co-substrate. The substrates were varied as follows: for TXN, 0–0.4 mM TS₂; for nsGPxA, 0–22 μ M TXN and 0–1 mM CumOOH; for TXNPx, 0–20 μ M TXN and 0–800 μ M CumOOH or 0–700 μ M t-butOOH. In these assays, the spurious reaction between the formed T(SH)₂ and the hydroperoxides was

monitored before the reaction was started, and subtracted when calculating the activity.

The thiol substrates were routinely calibrated using 5,5'-dithio-bis(2-nitrobenzoic acid), whereas ATP was calibrated using hexokinase and glucose-6-phosphate dehydrogenase. The experimental and coupling enzymes concentrations were varied to ensure that measurements were obtained under initial velocity conditions, except for TXNPx, which was measured under non-saturating conditions because of its instability under dilution.

Determination of enzyme activities in parasites under control and oxidant conditions

Forty million epimastigotes from the Querétaro strain [21] suspended in 1 mL of NaCl/P_i (137 mM NaCl, 2.7 mM KCl, 10 mM Na₂HPO₄ and 2 mM KH₂PO₄, pH 7.4) supplemented with 20 mM glucose were incubated at room temperature (25–30 °C) in the absence or presence of 50 μM H₂O₂. After 10 min, catalase (10 units) was added and further incubated for 2 min, and cytosolic extracts were obtained.

The cells were harvested, resuspended in 0.1 mL lysis buffer (20 mM Hepes, pH 7.4, 1 mM EDTA, 0.15 mM KCl, 1 mM dithiothreitol and 1 mM phenylmethanesulfonyl fluoride), and lysed by freezing in liquid nitrogen and thawing at 37 °C three times. The cellular extract was centrifuged at 20 817 *g* for 10 min, and the supernatant was immediately used for enzyme activity measurements. In the case of TXN and peroxidase activity, no pre-incubation in H₂O₂ was performed, i.e. the cells were harvested, washed in NaCl/P_i buffer, and lysed as described above.

γECS, GS and TryS activities in clarified cytosolic parasite extracts were determined by following ADP production in an end-point kinetic assay. Briefly, the reaction mixture contained 40 mM Hepes, pH 7.4, 10 mM MgCl₂, 0.1–0.5 mg cytosolic extract, and 1.3 mM Glu, 2.1 mM Cys and 2 mM ATP for γECS, 0.4 mM γEC, 8 mM Gly and 2 mM ATP for GS, and 8 mM GSH, 11 mM Spd, and 2 mM ATP for TryS. Parallel reactions were set up that lacked one of the co-substrates. After 30 min of incubation at 37 °C, the reaction was stopped by perchloric acid extraction (3% final concentration), the samples were centrifuged at 20 817 *g* for 10 min at 4 °C to eliminate the precipitated protein, and the supernatant was neutralized with 3 M KOH/0.1 M Tris. The ADP concentration was determined spectrophotometrically using a pyruvate kinase/lactate dehydrogenase-coupled assay as described previously [48]. The spurious ADP produced by ATPase activity in the clarified extracts in control reactions was always subtracted (Table S2). We ensured that the enzyme activity was linearly dependent on the amount of extract (Table S2). Longer incubation times decreased the enzyme activity. TryR activity was determined spectrophotometrically by following NADPH oxidation at 340 nm. The reaction mixture con-

tained 40 mM Hepes, pH 7.4, approximately 50 μg extract, 0.24 mM TS₂ and 0.2 mM NADPH. The TXN and peroxidase activities in the cytosolic parasite extracts were determined by reconstituting the antioxidant pathway in the same way as for the recombinant enzyme activities. The standard reaction mixture contained 40 mM Hepes, 1 mM EDTA, 0.16 mM NADPH, 0.5 μM TryR, 0.45 mM T(SH)₂ and 25–35 μg of parasite extract; subsequent additions were for TXN 0.1 mM CumOOH, and the reaction was started by adding 20 μM nsGPxA; for the TXN-dependent peroxidase activities were 6 μM CumOOH and the reaction was started by adding 20 μM TXN.

Determination of metabolites

For determination of thiol content, two protocols were used, either direct parasite mixing with perchloric acid or by preparing cytosolic extracts as described above, followed by incubation for 10 min on ice with an excess of NaBH₄, and further precipitation with 3% perchloric acid (final concentration). There were no differences in the results obtained using each protocol. The acid extracts were centrifuged at 20 817 *g* for 5 min at 4 °C. Twenty microlitres of the supernatant were separated by an HPLC system (Waters, Milford, MA, USA) coupled to a reversed-phase C18 column (3.5 μm particle size; Symmetry, Milford, MA, USA) previously equilibrated with a 99% trifluoroacetic acid solution (0.1% v/v in water) plus 1% acetonitrile. Thiol molecules were separated by elution with the same buffer for 10 min at a rate of 1 mL·min⁻¹; the eluates were mixed with 5,5'-dithio-bis(2-nitrobenzoic acid) and the absorbance was detected at 412 nm. The identity of each peak was determined using commercial compounds either run in parallel or mixed with the samples.

For TS₂ determination, approximately 1 × 10⁹ parasites were incubated for 10 min in the absence or presence of H₂O₂; the parasites were then harvested and resuspended in 0.025 mL buffer containing 40 mM Hepes, pH 8.0, 4 mM diethylenetriaminepentacetate and 6 mM *N*-ethylmaleimide. Alkylation of free thiols was performed at 70 °C for 3 min. An equal volume of 20% trichloroacetic acid in 10 mM HCl was added to the sample, which was further incubated for 30 min at 4 °C, followed by centrifugation at 20 817 *g* for 10 min at 4 °C. The unbound *N*-ethylmaleimide was extracted 10 times using water-saturated ethyl acetate, and the sample was bubbled with N₂. The acid extracts were neutralized using 3 M KOH/0.1 M Tris. The amount of TS₂ was determined in the neutralized extracts in a 1 mL reaction containing 40 mM Hepes, pH 7.4, 1 unit TryR and 0.16 mM NADPH. Alternatively, alkylation of free thiols using vinylpyridine was performed. Briefly, the same amount of parasites was deproteinized with 5% sulfosalicylic acid; then 2 μL 100% vinylpyridine were added, and the pH was adjusted to 6–7 by adding triethanolamine. The alkylation was performed at room temperature over 60 min, and TS₂

in the sample was quantified as described above. Both protocols yielded comparable results.

For determination of free amino acids, parasite extracts were obtained by three cycles of freezing and thawing, and perchloric acid was added for protein precipitation. The lysates were centrifuged at 20 817 *g* for 5 min at 4 °C, the supernatant was neutralized with 3 M KOH/0.1 M Tris, and the samples were derivatized with two volumes of an *ortho*-phthalaldehyde solution (7.4 mM *ortho*-phthalaldehyde, 5% ethanol, 5% β-mercaptoethanol and 9 mL 0.4 M boric acid, pH 10.4), and incubated for 3 min at room temperature. Fifty microlitres of the reaction were injected into an HPLC device coupled to a reversed-phase C18 column (Waters Spherisorb; 5 μm particle size; 4.6 × 250 mm column size) previously equilibrated with a mixture of 90% solution A (40 mM sodium phosphate buffer, pH 7.8) plus 10% solution B (45% methanol, 45% acetonitrile, 10% water). A 30 min gradient of solution B (10–90%) was used. The amino acids were detected by fluorescence (340 nm excitation, 460 nm emission).

For polyamine determination, the deproteinized cytosolic extracts were neutralized using NaHCO₃ powder, and the samples were evaporated at 70 °C. The desiccated samples were resuspended in a mix containing 0.080 mL 0.05 N HCl, 0.4 mL 0.1 M NaHCO₃, pH 9.15, and 0.8 mL 4 mM dansyl chloride, and incubated at 70 °C for 15 min; then 1 mL methanol was added for each 0.65 mL of sample, and the sample was filtered. Twenty microlitres were injected into an HPLC device coupled to a reversed-phase C18 column (Waters; 5 μm diameter Spherisorb; 4.6 × 250 mm column size) previously equilibrated with a mixture of 60% methanol and 40% water. A 23 min gradient from 60 to 95% methanol was used to separate the samples, and the polyamines were detected by fluorescence (365 nm excitation, 510 nm emission).

For ATP determination, deproteinized and neutralized cytosolic extracts were obtained as for amino acid content analysis from 2.4 × 10⁸ epimastigotes. ATP was determined as previously described [48]. NADP⁺ determination was performed by spectrofluorometry as described previously [75] from 2–3 × 10⁹ parasites. The NADPH concentration was calculated on the basis that the NADP/NADPH ratio in *T. cruzi* epimastigotes is 0.31 [76].

The metabolite concentrations were calculated by assuming that 1 × 10⁸ parasites correspond to 3 μL as described previously [77].

Flux determination

Aliquots of 4 × 10⁷ parasites resuspended in 1 mL NaCl/P; supplemented with 20 mM glucose were incubated at room temperature in the absence or presence of the peroxide; the cells were harvested at various times (0, 5 and 10 min), disrupted, and the T(SH)₂ content was determined by HPLC as described above. Flux was calculated considering that

1 × 10⁸ *T. cruzi* epimastigotes correspond to 0.23 ± 0.06 mg soluble protein (*n* = 5), value determined in the present study.

Rate equations used in the model

As the ATP concentration is high and constant under stress and non-stress conditions (Table 2), and is saturating (approximately 80-fold) for the three synthetic enzymes γECS, GS and TryS (Table 1), their rate equations were simplified by not including the ATP concentration. The *K_p* values used were the *K_i* values for the thiol product (Table 1). The *K_{eq}* values of 5597 used for the γECS, GS and TryS equations were calculated as described previously [39], in which Δ*G*^o (standard free energy change) was the difference between that of peptide bond formation (+2.2 kcal·mol⁻¹) and that of ATP hydrolysis (−7.3 kcal·mol⁻¹).

For γECS, a random bi-reactant rate equation with competitive inhibition by GSH versus Glu was used [78]:

$$v = \frac{V_{\max} \left((A * B) - \left(\frac{P}{K_{eq}} \right) \right)}{\left(1 + \left(\frac{A}{K_{mA}} \right) + \left(\frac{B}{K_{mB}} \right) + \left(\frac{A * B}{\alpha K_{mA} K_{mB}} \right) + \left(\frac{In}{K_i} \right) + \left(\frac{P}{K_{mP}} \right) + \left(\frac{A * In}{\beta K_i K_{mA}} \right) \right)}$$

where *A* = Cys, *B* = Glu, *In* = GSH and *P* is γEC. The α and β values were adjusted to reach metabolite concentrations present in the parasite (Tables S6 and S7). The α value is the factor by which binding of one substrate changes the affinity of the enzyme for the co-substrates. For γECS, the α value was 1, as previously reported [79]. The β value represents the factor by which the *K_m* for Cys is modified when GSH, which is an inhibitor, is bound to the free enzyme, competing for Glu. To our knowledge, no information on this value has been reported, thus it was adjusted to obtain the γEC concentrations in the parasite.

For GS, a random bi-reactant mechanism equation [78] was used:

$$v = \frac{V_{\max} \left((A * B) - \left(\frac{P}{K_{eq}} \right) \right)}{\left(1 + \left(\frac{A}{K_{mA}} \right) + \left(\frac{B}{K_{mB}} \right) + \left(\frac{P}{K_{mP}} \right) + \left(\frac{A * B}{\alpha K_{mA} K_{mB}} \right) \right)}$$

where *A* = γEC, *B* = Gly and *P* = GSH. An α value of 12 was used based on those obtained for *A. thaliana* GS [80].

*Tc*TryS is able to use GSH and free glutathionyl spermidine as substrates to synthesize T(SH)₂, but only the overall reaction was considered. For this enzyme, a random tri-uni mechanism equation was used [78]:

$$1 + 2 * \frac{V_{\max} \left((A * A * B) - \left(\frac{P}{K_{eq}} \right) \right)}{\alpha K_{mA} K_{mA} K_{mB}} + 2 * \left(\frac{A}{K_{mA}} + \frac{B}{K_{mB}} + \frac{A * A}{\alpha K_{mA} K_{mA}} \right) + 2 * \left(\frac{A * B}{\alpha K_{mA} K_{mB}} \right) + \left(\frac{A * A * B}{\alpha K_{mA} K_{mA} K_{mB}} \right) + \frac{P}{K_{mP}}$$

where *A* = GSH, *B* = Spd and *P* = T(SH)₂. As already mentioned, the *K_{m,GSH}* of *T. cruzi* TryS is 10 times higher

than the K_m reported for the *T. brucei* and *Leishmania* enzymes (Table S1). Thus, only when the α value was adjusted to a value of 0.1 (which increases the affinity for GSH by 10-fold) could the pathway kinetic model simulate the GSH concentration found in the parasites. This suggests the presence of an unknown TryS activator in *T. cruzi*.

The kinetic mechanism of TryR has not been described, but putative bi-bi-ping-pong kinetics have been suggested, similar to glutathione reductase [81]. To avoid adjustment of all the constants affecting the kinetic parameters for such a complex equation, its rate equation was simplified to ordered bi-bi kinetics [78]:

$$v = \frac{\frac{V_{\max}}{K_{mA}K_{mB}} \left((A * B) - \left(\frac{P * Q}{K_{eq}} \right) \right)}{\left(1 + \left(\frac{A}{K_{mA}} \right) + \left(\frac{B}{K_{mB}} \right) + \left(\frac{A * B}{K_{mA}K_{mB}} \right) + \left(\frac{P}{K_{mP}} \right) + \left(\frac{Q}{K_{mQ}} \right) + \left(\frac{P * Q}{K_{mP}K_{mQ}} \right) \right)}$$

where $A = \text{NADPH}$, $B = \text{TS}_2$, $P = \text{NADP}^+$ and $Q = \text{T(SH)}_2$.

For SpdT, a monosubstrate Haldane's equation [78] was used:

$$v = \frac{\frac{V_{\max}}{K_{mS}} * \left(S - \left(\frac{P}{K_{eq}} \right) \right)}{1 + \left(\frac{S}{K_{mS}} \right) + \left(\frac{P}{K_{mP}} \right)}$$

where $S = \text{Spd}_{\text{ext}}$ and $P = \text{Spd}_{\text{int}}$. The K_p and K_{eq} values were adjusted given that the Spd_{int} is low in the parasites and a high K_{eq} favours the forward reaction.

For the T(SH)_2 demand reaction, a reversible mass action equation was used:

$$v = k_1 \prod_i S_i - k_2 \prod_j P_j$$

For the reactions of the Spd, T(SH)_2 and GSH leaks, irreversible mass action equations were used:

$$v = k * \prod S_i$$

Acknowledgements

This work was supported by Consejo Nacional de Ciencia y Tecnología (CONACyT) Mexico grant numbers 83084 to E.S., and 80534 and 123636 to R.M.-S. V.O.-S. was supported by CONACyT PhD fellowship number 176966. We thank Professor Luise Krauth-Siegel Biochemistry Center, University of Heidelberg, Germany for providing T(SH)_2 for some experiments and accepting V.O.-S. for a short research stay at her laboratory.

References

- 1 World Health Organization (2007) *Reporte sobre la enfermedad de Chagas*. World Health Organization on behalf of the Special Programme for

Research and Training in Tropical Diseases, Geneva, Switzerland.

- 2 Coura JR & Albajar-Viñas P (2010) Chagas disease: a new worldwide challenge. *Nature* **465**, S6–S7.
- 3 Rodrigues J & de Castro SL (2002) A critical review on Chagas disease chemotherapy. *Mem Inst Oswaldo Cruz* **97**, 3–24.
- 4 Clayton J (2010) Chagas disease 101. *Nature* **465**, S4–S5.
- 5 Wilkinson SR & Kelly JM (2009) Trypanocidal drugs: mechanisms, resistance and new targets. *Expert Rev Mol Med* **11**, e31.
- 6 Fairlamb AH & Cerami A (1992) Metabolism and functions of trypanothione in the Kinetoplastida. *Annu Rev Microbiol* **46**, 695–729.
- 7 Krauth-Siegel RL & Comini MA (2008) Redox control in trypanosomatids, parasitic protozoa with trypanothione-based thiol metabolism. *Biochim Biophys Acta* **1780**, 1236–1248.
- 8 Irigoín F, Cibilis L, Comini MA, Wilkinson SR, Flohé L & Radi R (2008) Insights into the redox biology of *Trypanosoma cruzi*: trypanothione and oxidant detoxification. *Free Radic Biol Med* **45**, 733–742.
- 9 Olin-Sandoval V, Moreno-Sánchez R & Saavedra E (2010) Targeting trypanothione metabolism in trypanosomatid human parasites. *Curr Drug Targets* **11**, 1614–1630.
- 10 Taylor MC, Huang H & Kelly JM (2011) Genetic strategies in *Trypanosoma cruzi*. *Adv Parasitol* **75**, 231–250.
- 11 Krauth-Siegel L & Leroux AE (2012) Low molecular mass antioxidants in parasites. *Antioxid Redox Signal* doi:10.1089/ars.2011.4392.
- 12 Hornberg JJ, Bruggeman FJ, Bakker BM & Westerhoff HV (2007) Metabolic control analysis to identify optimal drug targets. *Prog Drug Res*, **64**, 171, 173–189.
- 13 Moreno-Sanchez R, Saavedra E, Rodríguez-Enríquez S, Gallardo-Pérez JC, Quezada H & Westerhoff HV (2010) Metabolic control analysis indicates a change of strategy in the treatment of cancer. *Mitochondrion* **10**, 626–639.
- 14 Klipp E, Wade RC & Kummer U (2010) Biochemical network-based drug-target prediction. *Curr Opin Biotechnol* **21**, 511–516.
- 15 Kolodkin A, Boogerd FC, Plant N, Bruggeman FJ, Goncharuk V, Lunshof J, Moreno-Sánchez R, Yilmaz N, Bakker BM, Snoep JL *et al.* (2011) Emergence of the silicon human and network targeting drugs. *Eur J Pharm Sci* doi:10.1016/j.ejps.2011.06.006.
- 16 Westerhoff HV & Palsson BO (2004) The evolution of molecular biology into systems biology. *Nat Biotechnol* **22**, 1249–1252.
- 17 Fell D (1997) *Understanding the Control of Metabolism*. Portland Press, London.
- 18 Moreno-Sanchez R, Saavedra E, Rodríguez-Enríquez S & Olin-Sandoval V (2008) Metabolic control analysis:

- a tool for designing strategies to manipulate metabolic pathways. *J Biomed Biotechnol* **2008**, 597913.
- 19 Snoep JL (2005) The Silicon Cell initiative: working towards a detailed kinetic description at the cellular level. *Curr Opin Biotechnol* **16**, 336–343.
 - 20 Westerhoff HV, Kolodkin A, Conradie R, Wilkinson SJ, Bruggeman FJ, Krab K, van Schuppen JH, Hardin H, Bakker BM, Moné MJ *et al.* (2009) Systems biology towards life *in silico*: mathematics of the control of living cells. *J Math Biol* **58**, 7–34.
 - 21 Bosseno MF, Barnabé C, Gastéllum EM, Kasten FL, Ramsey J, Espinoza B & Brenière SF (2002) Predominance of *Trypanosoma cruzi* lineage I in Mexico. *J Clin Microbiol* **40**, 627–632.
 - 22 Vanderheyden N, Benaïm G & Docampo R (1996) The role of a H⁺-ATPase in the regulation of cytoplasmic pH in *Trypanosoma cruzi* epimastigotes. *Biochem J* **318**, 103–109.
 - 23 Vanderheyden N & Docampo R (2000) Intracellular pH in mammalian stages of *Trypanosoma cruzi* is K⁺-dependent and regulated by H⁺-ATPases. *Mol Biochem Parasitol* **105**, 237–251.
 - 24 Oza SL, Tetaud E, Ariyanayagam MR, Warnon SS & Fairlamb AH (2002) A single enzyme catalyses formation of trypanothione from glutathione and spermidine in *Trypanosoma cruzi*. *J Biol Chem* **277**, 35853–35861.
 - 25 Oza SL, Ariyanayagam MR, Aitchison N & Fairlamb AH (2003) Properties of trypanothione synthetase from *Trypanosoma brucei*. *Mol Biochem Parasitol* **131**, 25–33.
 - 26 Oza SL, Shaw MP, Wyllie S & Fairlamb AH (2005) Trypanothione biosynthesis in *Leishmania major*. *Mol Biochem Parasitol* **139**, 107–116.
 - 27 Sharma SK & Banyal HS (2011) Characterization of *Plasmodium berghei* glutathione synthetase. *Parasitol Int* **60**, 321–323.
 - 28 Gupta S, Srivastava AK & Banu N (2005) *Setaria cervi*: kinetic studies of filarial glutathione synthetase by high performance liquid chromatography. *Exp Parasitol* **111**, 137–141.
 - 29 Volohonsky G, Tuby ANYH, Porat N, Wellman-Rousseau M, Visvikis A, Leroy P, Rashi S, Steinberg P & Stark AA (2002) A spectrophotometric assay of γ -glutamylcysteine synthetase and glutathione synthetase in crude extracts from tissues and cultured mammalian cells. *Chem Biol Interact* **140**, 49–65.
 - 30 Hell R & Bergmann L (1990) γ -glutamylcysteine synthetase in higher plants: catalytic properties and subcellular localization. *Planta* **180**, 603–612.
 - 31 Khan AU, Mei YH & Wilson T (1992) A proposed function for spermine and spermidine: protection of replicating DNA against damage by singlet oxygen. *Proc Natl Acad Sci USA* **89**, 11426–11427.
 - 32 Hernández SM, Sánchez MS & Schwarcz de Tarlovsky MN (2006) Polyamines as a defense mechanism against liperoxidation in *Trypanosoma cruzi*. *Acta Trop* **98**, 94–102.
 - 33 Wyllie S, Cunningham ML & Fairlamb AH (2004) Dual action of antimonial drugs on thiol redox metabolism in the human pathogen *Leishmania donovani*. *J Biol Chem* **279**, 39925–39932.
 - 34 Toledo I, Noronha-Dutra AA & Hansberg W (1991) Loss of NAD(P)-reducing power and glutathione disulfide excretion at the start of induction of aerial growth in *Neurospora crassa*. *J Bacteriol* **173**, 3243–3249.
 - 35 Sharma R, Awasthi S, Zimniak P & Awasthi YC (2000) Transport of glutathione-conjugates in human erythrocytes. *Acta Biochim Pol* **47**, 751–762.
 - 36 Mendes P (1993) GEPASI: a software package for modeling the dynamics, steady states and control of biochemical and other systems. *Comput Appl Biosci* **9**, 563–571.
 - 37 Hoops S, Sahle S, Gauges R, Lee C, Pahle J, Simus N, Singhal M, Xu L, Mendes P & Kummer U (2006) COPASI – a COMplex PATHway SIMulator. *Bioinformatics* **22**, 3067–3074.
 - 38 Cornish-Bowden A & Cárdenas ML (2001) Information transfer in metabolic pathways. Effects of irreversible steps in computer models. *Eur J Biochem* **268**, 6616–6624.
 - 39 Mendoza-Cózatl D & Moreno-Sánchez R (2006) Control of glutathione and phytochelatin synthesis under cadmium stress. Pathway modeling for plants. *J Theor Biol* **238**, 919–936.
 - 40 Hofmeyr JHS & Cornish-Bowden A (2000) Regulating the cellular economy of supply and demand. *FEBS Lett* **476**, 47–51.
 - 41 Krauth-Siegel RL, Enders B, Henderson GB, Fairlamb AH & Schirmer RH (1987) Trypanothione reductase from *Trypanosoma cruzi*. Purification and characterization of the crystalline enzyme. *Eur J Biochem* **164**, 123–128.
 - 42 Castro H & Tomás AM (2008) Peroxidases of trypanosomatids. *Antioxid Redox Signal* **10**, 1593–1606.
 - 43 van Gend C, Conradie R, du Preez FB & Snoep JL (2007) Data and model integration using JWS Online. *In Silico Biol* **7**, S27–S35.
 - 44 Rodríguez-Enríquez S, Carreño-Fuentes L, Gallardo-Pérez JC, Saavedra E, Quezada H, Vega A, Marín-Hernández A, Olin-Sandoval V, Torres-Márquez ME & Moreno-Sánchez R (2010) Oxidative phosphorylation is impaired by prolonged hypoxia in breast and possibly in cervix carcinoma. *Int J Biochem Cell Biol* **42**, 1744–1751.
 - 45 Marín-Hernández A, Gallardo-Pérez JC, Rodríguez-Enríquez S, Encalada R, Moreno-Sánchez R & Saavedra E (2011) Modeling cancer glycolysis. *Biochim Biophys Acta* **1807**, 755–767.
 - 46 Quezada H, Marín-Hernández A, Aguilar D, López G, Gallardo-Pérez JC, Jasso-Chávez R, González A,

- Saavedra E & Moreno-Sánchez R (2011) The Lys20 homocitrate synthase isoform exerts most of the flux control over the lysine synthesis pathway in *Saccharomyces cerevisiae*. *Mol Microbiol* **82**, 578–590.
- 47 Albert MA, Haanstra JR, Hannaert V, Van Roy J, Opperdoes FR, Bakker BM & Michels PA (2005) Experimental and *in silico* analyses of glycolytic flux control in bloodstream form *Trypanosoma brucei*. *J Biol Chem* **280**, 28306–28315.
- 48 Saavedra E, Marín-Hernández A, Encalada R, Olivos A, Mendoza-Hernández G & Moreno-Sánchez R (2007) Kinetic modeling can describe *in vivo* glycolysis in *Entamoeba histolytica*. *FEBS J* **274**, 4922–4949.
- 49 Moreno-Sánchez R, Encalada R, Marín-Hernández A & Saavedra E (2008) Experimental validation of metabolic pathway modeling. *FEBS J* **275**, 3454–3469.
- 50 Sousa M, Ferreira AE, Tomás AM, Cordeiro C & Ponces A (2005) Quantitative assessment of the glyoxylase pathway in *Leishmania infantum* as a therapeutic target by modelling and computer simulation. *FEBS J* **272**, 2388–2398.
- 51 Grondin K, Haimeur A, Mukhopadhyay R, Rosen BP & Ouellette M (1997) Co-amplification of the γ -glutamylcysteine synthetase gene *gsh1* and of the ABC transporter gene *pgpA* in arsenite-resistant *Leishmania tarentolae*. *EMBO J* **16**, 3057–3065.
- 52 Guimond C, Trudel N, Brochu C, Marquis N, El Fadili A, Peytavi R, Briand G, Richard D, Messier N, Papadopoulou B *et al.* (2003) Modulation of gene expression in *Leishmania* drug resistant mutants as determined by targeted DNA microarrays. *Nucleic Acids Res* **31**, 5886–5896.
- 53 Mukherjee A, Padmanabhan OK, Singh S, Roy G, Giraard I, Chatterjee M, Ouellette M & Madhubala R (2007) Role of ABC transporter MRPA, γ -glutamylcysteine synthetase and ornithine decarboxylase in natural antimony-resistant isolates of *Leishmania donovani*. *J Antimicrob Chemother* **59**, 201–211.
- 54 Wyllie S, Mandal G, Singh N, Sundar S, Fairlamb AH & Chatterjee M (2010) Elevated levels of tryparedoxin peroxidase in antimony unresponsive *Leishmania donovani* field isolates. *Mol Biochem Parasitol* **173**, 162–164.
- 55 Opperdoes FR & Michels PA (2001) Enzymes of carbohydrate metabolism as potential drug targets. *Int J Parasitol* **31**, 482–490.
- 56 Saavedra E, Encalada R, Pineda E, Jasso-Chávez R & Moreno-Sánchez R (2005) Glycolysis in *Entamoeba histolytica*. Biochemical characterization of recombinant glycolytic enzymes and flux control analysis. *FEBS J* **272**, 1767–1783.
- 57 Huynh TT, Huynh VT, Harmon MA & Phillips MA (2003) Gene knockdown of γ -glutamylcysteine synthetase by RNAi in the parasitic protozoa *Trypanosoma brucei* demonstrates that it is an essential enzyme. *J Biol Chem* **278**, 39794–39800.
- 58 Mukherjee A, Roy G, Guimond C & Ouellette M (2009) The γ -glutamylcysteine synthetase gene of *Leishmania* is essential and involved in response to oxidants. *Mol Microbiol* **74**, 914–927.
- 59 Faundez M, Pino L, Letelier P, Ortiz C, Lopez R, Seguel C, Ferreira J, Pavani M, Morello A & Maya JD (2005) Buthionine sulfoximine increases the toxicity of nifurtimox and benznidazole to *Trypanosoma cruzi*. *Antimicrob Agents Chemother* **49**, 126–130.
- 60 Faundez M, Lopez-Munoz R, Torres G, Morello A, Ferreira J, Kemmerling U, Orellana M & Maya JD (2008) Buthionine sulfoximine has anti-*Trypanosoma cruzi* activity in a murine model of acute Chagas' disease and enhances the efficacy of nifurtimox. *Antimicrob Agents Chemother* **52**, 1837–1839.
- 61 Torrie LS, Wyllie S, Spinks D, Oza SL, Thompson S, Harrison JR, Gilbert IH, Wyatt PG, Fairlamb AH & Frearson JA (2009) Chemical validation of trypanothione synthetase: a potential drug target for human trypanosomiasis. *J Biol Chem* **284**, 137–145.
- 62 Frearson JA, Wyatt PG, Gilbert IH & Fairlamb AH (2007) Target assessment for antiparasitic drug discovery. *Trends Parasitol* **23**, 589–595.
- 63 Comini MA, Guerrero SA, Haile S, Menge U, Lündsdorf H & Flohé L (2004) Validation of *Trypanosoma brucei* trypanothione synthetase as drug target. *Free Radic Biol Med* **36**, 1289–1302.
- 64 Ariyanayagam MR, Oza SL, Guther ML & Fairlamb AH (2005) Phenotypic analysis of trypanothione synthetase knockdown in the African trypanosome. *Biochem J* **391**, 425–432.
- 65 Le Quesne SA & Fairlamb AH (1996) Regulation of a high-affinity diamine transport system in *Trypanosoma cruzi* epimastigotes. *Biochem J* **316**, 481–486.
- 66 Carrillo C, Canepa GE, Algranati ID & Pereira CA (2006) Molecular and functional characterization of a spermidine transporter (TcPAT12) from *Trypanosoma cruzi*. *Biochem Biophys Res Commun* **344**, 936–940.
- 67 Gonzalez NS, Ceriani C & Algranati ID (1992) Differential regulation of putrescine uptake in *Trypanosoma cruzi* and other trypanosomatids. *Biochem Biophys Res Commun* **188**, 120–128.
- 68 Hasne MP, Coppens I, Soysa R & Ullman B (2010) A high-affinity putrescine-cadaverine transporter from *Trypanosoma cruzi*. *Mol Microbiol* **76**, 78–91.
- 69 Algranati ID (2010) Polyamine metabolism in *Trypanosoma cruzi*: studies on the expression and regulation of heterologous genes involved in polyamine biosynthesis. *Amino Acids* **38**, 645–651.
- 70 Persson L (2007) Ornithine decarboxylase and S-adenosylmethionine decarboxylase in trypanosomatids. *Biochem Soc Trans* **35**, 314–317.
- 71 Dumas C, Ouellette M, Tovar J, Cunningham ML, Fairlamb AH, Tamar S, Olivier M & Papadopoulou B (1997) Disruption of the trypanothione reductase gene

- of *Leishmania* decreases its ability to survive oxidative stress in macrophages. *EMBO J* **16**, 2590–2598.
- 72 Krieger S, Schwarz W, Ariyanayagam MR, Fairlamb AH, Krauth-Siegel RL & Clayton C (2000) Trypanosomes lacking trypanothione reductase are avirulent and show increased sensitivity to oxidative stress. *Mol Microbiol* **35**, 542–552.
- 73 Fernández-Presas AM, Tato P, Becker I, Solano S, Kopitin N, Berzunza M, Willms K, Hernández J & Molinari JL (2010) Specific antibodies induce apoptosis in *Trypanosoma cruzi* epimastigotes. *Parasitol Res* **106**, 1327–1337.
- 74 Berzunza-Cruz M, Cabrera N, Crippa-Rossi M, Sosa Cabrera T, Pérez-Montfort R & Becker I (2002) Polymorphism analysis of the internal transcribed spacer and small subunit of ribosomal RNA genes of *Leishmania mexicana*. *Parasitol Res* **88**, 918–925.
- 75 Bergmeyer HU (1985) *Methods of Enzymatic Analysis*, Vol. VI, 3rd edn. Deutsche Bibliothek, Federal Republic of Germany.
- 76 De Vas MG, Portal P, Alonso GD, Schlesinger M, Flawia MM, Torres HN, Fernández-Villamil S & Paveto C (2011) The NADPH-cytochrome P450 reductase family in *Trypanosoma cruzi* is involved in the sterol biosynthesis pathway. *Int J Parasitol* **41**, 99–108.
- 77 Rangel-Aldao R, Allende O, Triana F, Piras R, Henriquez D & Piras M (1987) Possible role of cAMP in the differentiation of *Trypanosoma cruzi*. *Mol Biochem Parasitol* **22**, 39–43.
- 78 Segel IH (1975) *Enzyme Kinetics*. Wiley, New York.
- 79 Brekken DL & Phillips MA (1998) *Trypanosoma brucei* γ -glutamylcysteine synthetase. Characterization of the kinetic mechanism and the role of Cys-319 in cystamine inactivation. *J Biol Chem* **273**, 26317–26322.
- 80 Jez JM & Cahoon RE (2004) Kinetic mechanism of glutathione synthetase from *Arabidopsis thaliana*. *J Biol Chem* **279**, 42726–42731.
- 81 Montero S, de Arriaga D & Soler J (1990) A study of kinetic mechanism followed by glutathione reductase from mycelium of *Phycomyces blakesleeanus*. *Arch Biochem Biophys* **278**, 52–59.
- 82 Marton LJ, Russell DH & Levy CC (1973) Measurement of putrescine, spermidine and spermine in physiological fluids by use of an amino acid analyzer. *Clin Chem* **19**, 923–926.
- 83 Bitonti AJ, Kelly SE & McCann PP (1984) Characterization of spermidine synthase from *Trypanosoma brucei*. *Mol Biochem Parasitol* **13**, 21–28.
- 84 Basselin M, Coombs GH & Barrett MP (2000) Putrescine and spermidine transport in *Leishmania*. *Mol Biochem Parasitol* **109**, 37–46.

Supporting information

The following supplementary material is available:

Fig. S1. SDS/PAGE of the purified enzymes.

Fig. S2. Kinetics of *TcTryS* against GSH.

Fig. S3. γ ECS inhibition by GSH and γ EC.

Fig. S4. Dependence of flux and T(SH)₂ concentration on the *k* values of the leaks.

Table S1. Comparison of the kinetic parameters of the pathway enzymes with those reported in the literature.

Table S2. Determination of GS and TryS activities in parasite extracts.

Table S3. Enzyme activities in parasite extracts exposed to various conditions.

Table S4. Thiol content in various strains of *Trypanosoma cruzi* epimastigotes.

Table S5. Reactions as written in GEPASI/COPASI.

Table S6. Summary of the rate constant values used in the model.

Table S7. Summary of the affinity values used for each enzyme.

Table S8. Robustness of the model.

Table S9. Elasticity coefficients.

This supplementary material can be found in the online version of this article.

Please note: As a service to our authors and readers, this journal provides supporting information supplied by the authors. Such materials are peer-reviewed and may be re-organized for online delivery, but are not copy-edited or typeset. Technical support issues arising from supporting information (other than missing files) should be addressed to the authors.